land

MDPI

Article

Snow Avalanche Assessment in Mass Movement-Prone Areas: Results from Climate Extremization in Relationship with Environmental Risk Reduction in the Prati di Tivo Area (Gran Sasso Massif, Central Italy)

Massimiliano Fazzini [1], Marco Cordeschi [2], Cristiano Carabella [1], Giorgio Paglia [1], Gianluca Esposito [1] and Enrico Miccadei [1,*]

[1] Department of Engineering and Geology, Università degli Studi "G. d'Annunzio" Chieti-Pescara, Via dei Vestini 31, 66100 Chieti Scalo, Italy; massimiliano.fazzini@unich.it (M.F.); cristiano.carabella@unich.it (C.C.); giorgio.paglia@unich.it (G.P.); gianluca.esposito@unich.it (G.E.)
[2] Altevie Engineering, Viale Francesco Crispi 19/b, 67100 L'Aquila, Italy; cordeschi@altevie.eu
* Correspondence: enrico.miccadei@unich.it

Abstract: Mass movements processes (i.e., landslides and snow avalanches) play an important role in landscape evolution and largely affect high mountain environments worldwide and in Italy. The increase in temperatures, the irregularity of intense weather events, and several heavy snowfall events increased mass movements' occurrence, especially in mountain regions with a high impact on settlements, infrastructures, and well-developed tourist facilities. In detail, the Prati di Tivo area, located on the northern slope of the Gran Sasso Massif (Central Italy), has been widely affected by mass movement phenomena. Following some recent damaging snow avalanches, a risk mitigation protocol has been activated to develop mitigation activities and land use policies. The main goal was to perform a multidisciplinary analysis of detailed climatic and geomorphological analysis, integrated with Geographic Information System (GIS) processing, to advance snow avalanche hazard assessment methodologies in mass movement-prone areas. Furthermore, this work could represent an operative tool for any geomorphological hazard studies in high mountainous environments, readily available to interested stakeholders. It could also provide a scientific basis for implementing sustainable territorial planning, emergency management, and loss-reduction measures.

Keywords: snow avalanche; mass movements-prone areas; hazard assessment; climate extremization; environmental risk; Gran Sasso Massif; Central Apennines

check for updates

Citation: Fazzini, M.; Cordeschi, M.; Carabella, C.; Paglia, G.; Esposito, G.; Miccadei, E. Snow Avalanche Assessment in Mass Movement-Prone Areas: Results from Climate Extremization in Relationship with Environmental Risk Reduction in the Prati di Tivo Area (Gran Sasso Massif, Central Italy). *Land* **2021**, *10*, 1176. https://doi.org/10.3390/land10111176

Academic Editor: Giulio Iovine

Received: 8 October 2021
Accepted: 29 October 2021
Published: 2 November 2021

Publisher's Note: MDPI stays neutral with regard to jurisdictional claims in published maps and institutional affiliations.

Copyright: © 2021 by the authors. Licensee MDPI, Basel, Switzerland. This article is an open access article distributed under the terms and conditions of the Creative Commons Attribution (CC BY) license (https://creativecommons.org/licenses/by/4.0/).

1. Introduction

Mass movement phenomena (i.e., rockfalls, debris flows, shallow landslides, snow avalanches, etc.) play a significant role in the landscape evolution and occur in relation to physiographic, geomorphological, and climatic features and to triggering effects induced by human and/or seismic activity [1–12]. These phenomena cause significant disasters on a global scale every year, and the frequency of their occurrence seems to be on the rise. The expansion of urbanization and the tourism development in particular areas, such as mountainous regions, notably increased the environmental hazards and risks. Moreover, climate extremization and the potential for more severe weather conditions could also be acknowledged as contributing factors. Hence, these events can significantly impact mountain environments, residential areas in avalanche zones, ecosystems, and public infrastructures [13,14].

According to the Emergency Events Database—EMDAT [15], snowfall and snow avalanches are considered natural hazards belonging to hydrometeorological events. Snow avalanches are critical events connected to the sudden instability of snow-covered slopes in geodynamical active mountain regions. Moreover, they are undoubtedly one of the major

denudational processes in cold and mountainous areas, representing a huge natural hazard with devastating socioeconomic and environmental impacts [16,17].

Mass movement triggering is linked to sudden changes in the geomorphological features of the slopes and the physical characteristics of the snow cover [18,19], resulting, in turn, from numerous variables in continuous changes, such as the geomorphological characteristics of the site, the static and dynamic climatological trends, the processes of metamorphism of the snowy mantle, and the effects of new snow overloading on a preexisting snow cover caused by the action of wind and seismic events of significant magnitude.

It is crucial to follow different approaches to map snow avalanches to provide correct and valuable hazard assessments. Hazard maps represent significant and essential tools needed to evaluate snow avalanche susceptibility of an area, such as a ski resort [20]. It is possible to distinguish between different types of avalanche hazard maps: inventory maps, such as France Carte de Localisation Probable des Avalanches CLPA, [21], depicting the maximum extends of known avalanches, usually compiled from literature, technical documents, and interviews and supported by air–photo interpretation and field investigations and hazard maps [22,23], outlining zones affected by different degrees of hazard, generally drawn based on known historical events, geomorphological studies, and statistical and/or dynamic computational models. In addition to these thematic maps, several techniques can be used to evaluate avalanche hazards and risks involving the implementation of defense structures, closures, and explosives [24,25]. Since the pioneering works in this research field [26,27], most studies were performed to evaluate the long-term risk on settlements and critical infrastructure. These authors all used solid explosives, investigated shock waves propagating through a snowpack, and showed the distinct damping effect of snow, e.g., [28–30]. According to the literature and technical reports [31–33], the techniques used to evaluate avalanche hazards and risks are different depending on the circumstances. The long-term risk affecting permanent settlements and critical infrastructure is typically managed by conducting hazard mapping during the main steps of the land planning process. On the other side, safety services for ski resorts, ski facilities, and temporary worksites are characterized by closures and explosives (i.e., Obellx® gas exploder) to manage short-term avalanche risk; guides adopt professional route selection to control the exposure of people, and public avalanche forecasters communicate regional avalanche danger to a direct stakeholder who manages their own risk [16].

Moreover, it must be considered that the devastating propagation of a snow avalanche may contribute to the mass wasting of rocks and vegetation being transported along the way and accumulated together with the snow avalanche debris. This induced mass wasting poses longer-lasting damages with more destructive effects [34]. As a result, to completely define the degree of hazard in mass movement-prone areas, dynamic computational models can help to estimate paths and impact pressures in the runout zone [35]. Modeling the avalanche triggering mechanisms is complicated, and this complexity has been widely described in many studies [36,37]. The morphological setting (i.e., terrain and slope), the snowpack, and the meteorological conditions contribute to the avalanche movement and propagation. Based on the interaction of these parameters, the avalanche formation and its propagation can eventually be modeled [38–42]. The models have been largely enhanced with the involvement of recent advanced technologies of Geographic Information Systems (GIS) [43–45], which have become powerful tools for the implementation of required databases to support decision-making activities in land planning, such as over hazardous regions posed as a threat by several geohazards (i.e., landslides and snow avalanches).

The mountain territories of the Abruzzo Region are not immune to the general phenomenon of increased tourists' fruition and related snow avalanche risk. Nevertheless, due to its geographical location and physiographic framework (Figure 1), the Abruzzo Region also shows peculiar meteorological and snow characteristics that differ from the rest of the Alps and Central Apennines [46].

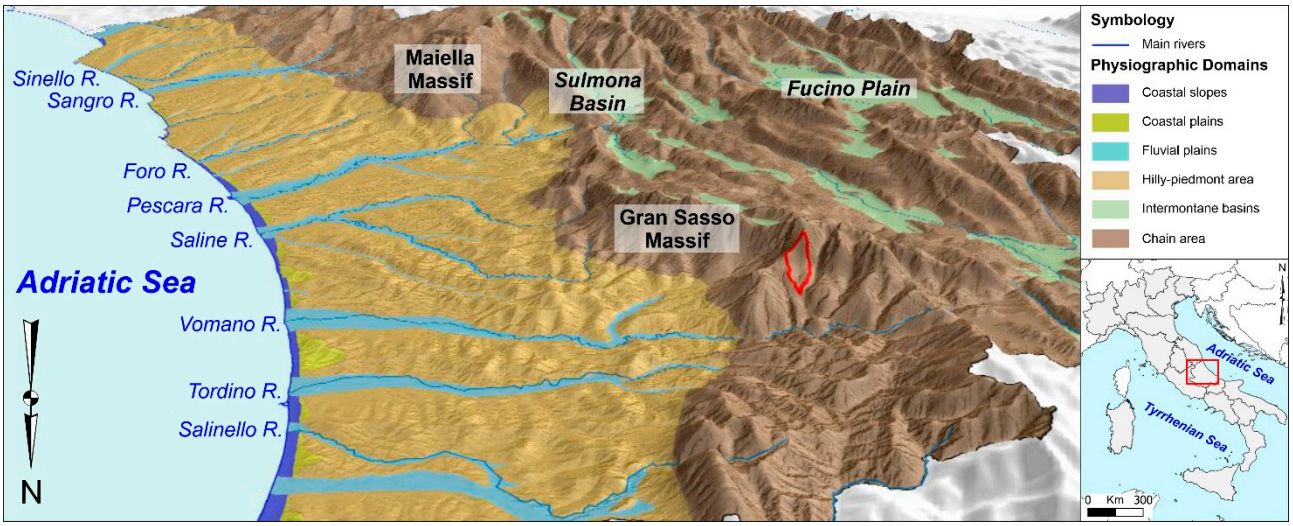

Figure 1. Three-dimensional view (from 20 m DTM, SINAnet) of the Abruzzo Region (Central Italy) and main physiographic domains. The red polygon indicates the study area.

The study area is located in the northeastern part of the Abruzzo Region within the Gran Sasso Massif (Figure 1). It is sited in the municipal territory of Pietracamela. It includes, to the south, a wide irregular mountainous landscape dominated by the Corno Grande (2912 m a.s.l.), featuring as the highest peak of the Apennines Chain.

To develop the present study, an integrated and multidisciplinary approach was followed to provide further advancement in snow avalanche hazard assessment methodologies. Combining and integrating morphometric, geomorphological, climatic, and nivological analyses, it was possible to better define the existing relationships between climate extremization and environmental risk reduction in a mass movement-prone area, such as the Prati di Tivo area. This paper focuses on the stepwise approach for a correct snow avalanche assessment by combining the patterns of snow avalanches and the main meteorological features of the study area. Morphometric and geomorphological analyses were carried out to evaluate landslide hazards in this mass movement-prone area, mainly focusing on the dynamic geomorphic action of snow avalanches. The role of the geomorphological and climatic features in the triggering of the avalanches was also evaluated. Furthermore, it describes the safety services and the risk mitigation protocol to perform over a ski facilities area in such a mass movement-prone setting. This work could represent an effective tool in geomorphological hazard studies for high mountainous environments readily available to interested stakeholders, which provides a scientific basis for territorial planning, emergency management, and mitigation measures.

2. Study Area

2.1. Geological and Geomorphological Setting

The study area is located in Central Italy within the northern sector of the Abruzzo Region, and it is strictly located in the Apennines Chain area, showing a high-relief mountainous landscape. The Central Apennines chain's morphology is characterized by the presence of a series of ridges trending from NW–SE to N–S (i.e., Gran Sasso Massif, 2912 m a.s.l.; Maiella Massif, 2793 m a.s.l.), separated by longitudinal and transversal valleys and broad intermontane basins (elevation 250–1000 m a.s.l.—i.e., Fucino Plain and Sulmona Basin) (Figure 1). The elevation abruptly drops down to the hilly piedmont area (ranging from ~800 m a.s.l. to the coastline), which features a mesa, cuesta, and plateau landscape [47–50]. The northeastern front of the asymmetric Abruzzo Apennines chain is characterized by a steep mountainside with large escarpments. The Gran Sasso Massif is the highest in the Central Apennines, with several peaks above 2500 m a.s.l. It features an

arched shape, trending from W–E to N–S, and drops down to lower elevations (>1000 m a.s.l.), defining a large and steep mountain escarpment.

The chain is composed of pre-orogenic lithological sequences that belong to different Meso–Cenozoic paleogeographic domains (carbonate ramp and platform limestones and slope-to-pelagic limestones). The Neogene deformation of these sequences, along NW–SE to N–S-oriented (W-dipping) thrusts, determined the emplacement of the main mountain ridges, also including the Gran Sasso one (Figure 2) [51–58].

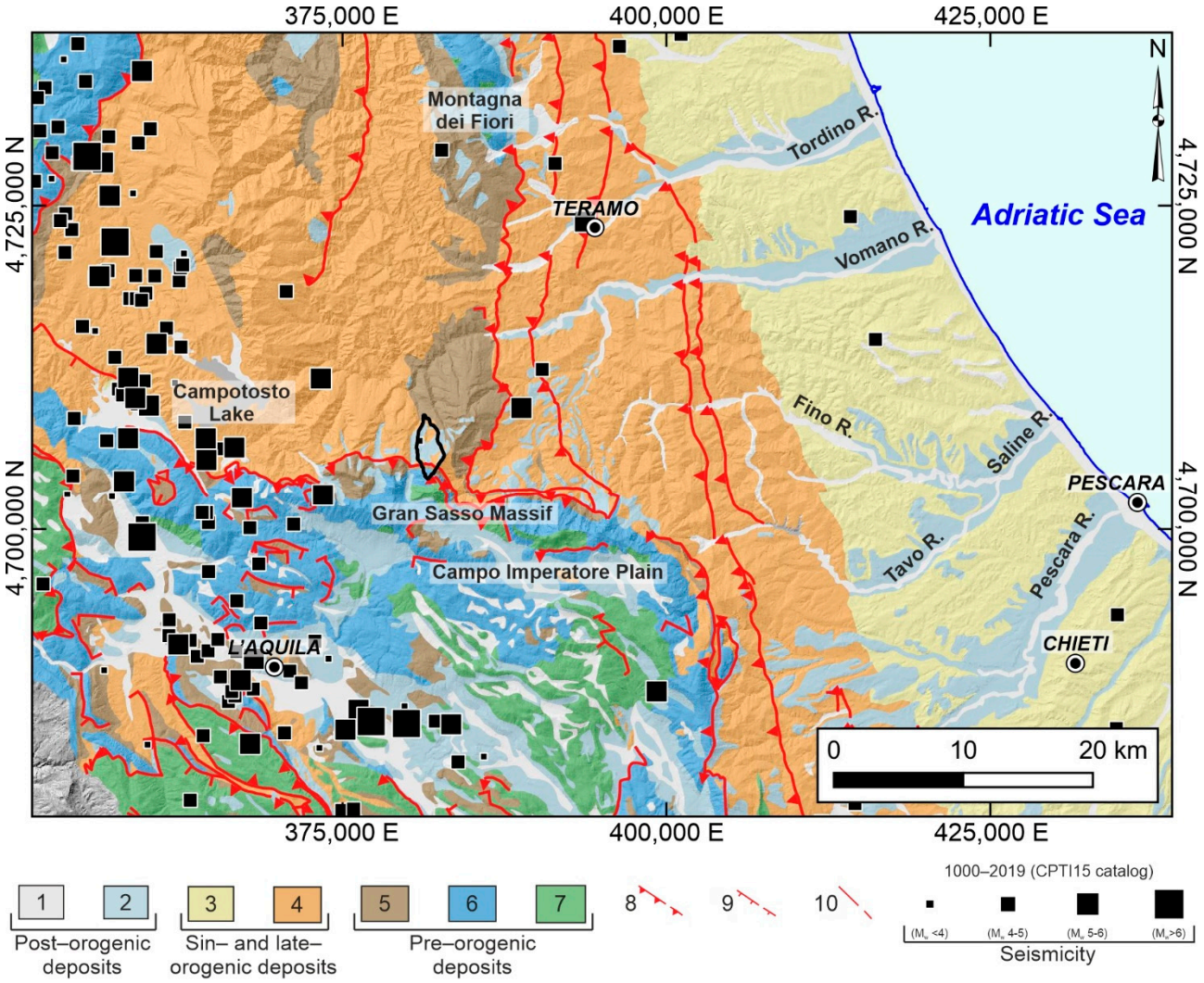

Figure 2. Geological map of NE Abruzzo (modified from [59]). Legend: post-orogenic deposits—(1) fluvial deposits (Holocene) and (2) fluvial and alluvial fan deposits (Middle-Late Pleistocene); sin- and late-orogenic deposits—(3) hemipelagic sequences with conglomerate levels (Late Pliocene–Early Pleistocene) and (4) turbiditic foredeep sequences (Late Miocene–Early Pliocene); pre-orogenic deposits—(5) carbonate ramp facies (Early Miocene-Early Pliocene), (6) slope and pelagic basin sequences (Cretaceous–Miocene), and (7) carbonate platform sequences (Jurassic–Miocene); (8) major thrust (dashed if buried); (9) major normal fault (dashed if buried); and (10) major fault with strike-slip or reverse component (dashed if buried). Seismicity derived from the CPTI15 catalog [60]. The black line indicates the location of the study area.

This compressional phase was followed by extensional and strike-slip tectonics along mostly the NW–SE to NNW–SSE-oriented faults, which define the present-day landscape configuration [47,61,62]. The hilly piedmont and coastal areas are made up of sin- and late-orogenic deposits (i.e., sandy-pelitic turbiditic foredeep sequences), largely covered and unconformably overlaid by Pleistocene hemipelagic sequences. The post-orogenic

deposits mainly consist of fluvial and alluvial fan deposits, as well as glacial, travertine, slope, and eluvial–colluvial deposits (Figure 2).

The geomorphological framework is mainly related to mass wasting; gravity-induced (e.g., mostly rotational–translational slides, earth flows, rockfalls, and complex slides); and fluvial-related (e.g., debris flows, alluvial fans, etc.) processes. Ancient glacial processes are preserved as relict landforms [48,63–66].

According to the historical and instrumental data [67–69], Central Italy has been affected by many earthquakes, with recurrent seismic events of moderate-to-high intensity. The present-day regional tectonic setting is dominated by intense seismicity (up to Mw 7.0 [60]), with earthquakes mostly located in the chain sectors (i.e., 2009, L'Aquila and 2016–2017, Central Italy); moderate seismicity also affects the hilly piedmont and Adriatic areas.

2.2. Climatic Setting

The Abruzzo Region climate is affected by the physiographic and morphological setting of the Central Apennine Chain and its eastern front in the proximity of the upper watershed divide. This geographic position, located not far from the Adriatic Sea—approximately 40 km as the crow flies—largely influences the climate setting, varying from a Mediterranean type along the coasts and the hilly piedmont areas to a more temperate and continental type in the chain area [70,71]. The morphological arrangement also regulates the rainfall distribution; the highest annual rainfall values (up to 1500–2000 mm/y) occur along the main ridges and in the inland sectors, decreasing down to ~600 mm/year along the hilly piedmont and coastal areas. It is occasionally characterized by heavy rainfall events (>100 mm/d and 30–40 mm/h) [72–74]. The average temperature values range between 8 and 10 °C in the mountain sectors (average minimum values of 0–5 °C at high elevations) and between 16 and 18 °C along the coast. The winter temperature (average January values) shows low values in the inland areas (0–2 °C, with minimum values of approximately −5 to −10 °C at high elevations) and higher ones (8–10 °C) in the hilly piedmont sectors. Over the past two decades, the Abruzzo Region has been affected by some heavy rainfall events and snowstorms, generated by heavy rainfall ranging from 60 to 100 mm in a few hours to >200 mm per day and by snowfall up to >100 cm/day (e.g., January 2003, April 2004, October 2007, March 2011, September 2012, December 2013, February-March 2015, and January-February 2017 [75]).

More in detail, the mountainous landscape and the homogeneous aspect exposure distribution with north exposed slopes determines a harsh climate poorly mitigated by the maritime influence, as confirmed by the presence of the Calderone glacier—the southernmost one in Europe [64,76].

The Abruzzo Apennine chain sector represents an orographic barrier able to strongly diversify the effects of atmospheric currents on its slopes, with upwind (Stau) and downwind (Föhn or, locally, "Garbino") flows that rule and modify the spatial and altitudinal distributions of rainfall and snowfall events [77,78]. Inland sectors, according to their upwind exposure to cold polar currents moisture-laden after transit through the Adriatic and/or Tyrrhenian sides, are characterized by intense and frequent rainfall events [79]. Furthermore, even if, in such a climatically dynamic framework, it is not uncommon to detect minimum winter temperatures around −25 °C, the Central Apennines (i.e., Abruzzo and Molise regions) show geomorphological situations that determine the presence of a cold air pool. About this, the absolute minimum values were recorded in recent times in several intermontane plains at an elevation ranging from 1200 to 1500 m a.s.l., such as the Piane di Pezza Plain (−37.4 °C), Cinquemiglia Plain (−30 °C), Campo Felice Plain (−32 °C), and Marsia Plain (−36 °C) [80].

According to previous analyses and data [70,71,81,82], the study area is characterized by transitional thermal–meteoric features that largely influence the climate setting varying from continental sub-Apennine to sub-Mediterranean Apennine regimes, considering its

southern latitudinal location and the relatively small distance from the Adriatic Sea, which exerts a strong maritime influence.

3. Materials and Methods

The study area was investigated through an integrated and multidisciplinary approach (Figure 3) based on (i) a morphometric analysis, (ii) geomorphological analysis, (iii) climatic analysis, (iv) nivological analysis, and (v) analysis for the assessment of snow avalanche hazard, supported by the combination of literature data and GIS-based techniques.

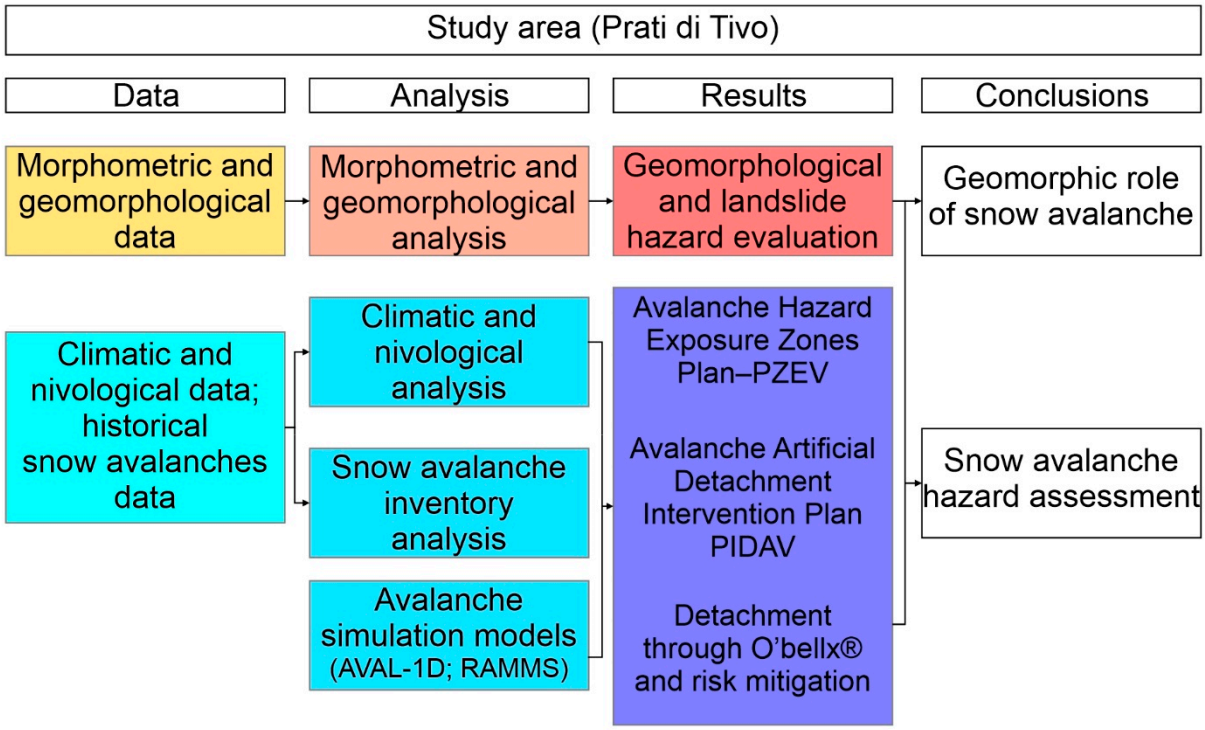

Figure 3. Schematic flowchart diagram showing the main methodological steps.

3.1. Morphometric Analysis

The analysis was performed using topographic maps (1:25,000–1:5000 scale) and supported by the creation of a Digital Elevation Model (5-m DEM) derived from 1:5000 scale regional technical maps, previously retrieved from Open Geodata Portal of the Abruzzo Region (http://opendata.regione.abruzzo.it/, accessed on 15 May 2021). It was carried out in Geographic Information System (GIS) software (QGIS 2020, version 3.16 "Hannover"). It was centered on the definition of the main physiographic features of the study area in order to highlight the morphological setting of this high mountainous environment quantitatively. In detail, the analysis was based on the computation of three main parameters: elevation, slope (first derivate of elevation [83]), and local relief. This latter was calculated as the elevation range within 1 × 1 km windows, according to Ahnert [84].

According to Schweizer et al. [85], snow avalanche formations result from the complex interaction between the topography, snowpack, and meteorological conditions. As a result, the morphometric characteristics (i.e., slope aspect, relative slope height, and slope inclination of the snow avalanche) are seen as most important in determining the spatial patterns of snow accumulation and, accordingly, the starting, transition, and runout zones [86]. Looking at the landscape parameters evaluated for the study area, the computed morphometric factors (elevation, slope, and local relief) appear to be the most relevant, which control the spatial distribution of snow avalanche activity.

The study area is strictly located to the main drainage basin, automatically extracted from the DEM using the Hydrological Tools in QGIS, whose closing point was located at

Pietracamela Village (Figure 4). This assumption was followed in order to have a basic unit to which to refer to in performing all the multidisciplinary analyses, revealing that the drainage basin scale may be the most convenient choice [87].

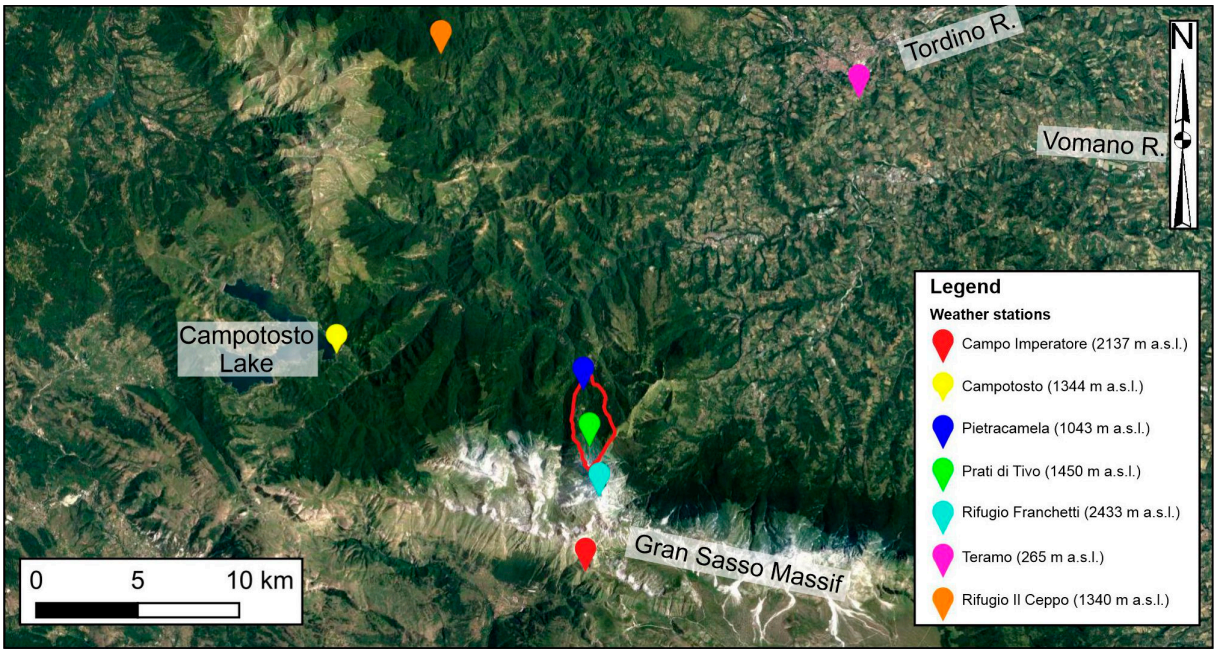

Figure 4. Spatial distribution of the weather gauges used in the present study. The red line indicates the location of the study area.

3.2. Geomorphological Analysis

This analysis involved preliminary storing and managing existing data, retrieved from public authorities' technical reports, databases, and the scientific literature. Specifically, geological–geomorphological data were supplied by the CARG Project-Sheet 349 "Gran Sasso d'Italia" [88], the Abruzzo-Sangro Basin Authority [89], the IFFI database [90], and scientific publications [47,65]. These data were integrated and verified through geomorphological field mapping, carried out at an appropriate scale (1:5000–1:10,000), and stereoscopic air photo interpretation using 1:33,000- and 1:10,000-scale stereoscopic air photos (Flight GAI 1954 and Flight Abruzzo Region 1981–1987), as well as an analysis of 1:5000-scale orthophoto color images (Flight Abruzzo Region 2010) and Google Earth® imagery (2019–2020). Field mapping was focused on the definitions of the lithological features and geomorphological landforms, with reference to the main mass movements affecting the study area. It was performed according to the Italian geomorphological guidelines [91], international guidelines [92], and thematic literature concerning geomorphological mapping and analysis in different geological and climatic contexts, as well as field-based and numerical analysis [93–97].

3.3. Climatic Analysis

Climatic data analysis was carried out to outline the distribution of the climatic parameters and conditions in the study area. The analysis was based on a dataset obtained from a network of 7 gauges (colored dots in Figure 4; data provided by the Functional Center and Hydrographic Office of the Abruzzo Region and the *amateur meteorological association* L'Aquila Caput Frigoris—https://www.caputfrigoris.it/, accessed on 12 January 2021). More in detail, according to the lack of historical thermo–pluviometric series suiting the World Meteorological Organization (WMO) directives [98], climatic data belonging to the Pietracamela gauge (1043 m a.s.l.; blue dot in Figure 4) were used to quantify the microclimatic setting of the study area properly. Its dataset gathers thermo–pluviometric

series data covering a 50-year time record (1950–2004). Recently, three gauges, featuring technical elements in accordance with the WMO 1083 directives [98], were located at the Teramo (265 m a.s.l.; pink dot in Figure 4), near the tourist and ski facilities at Prati di Tivo (1450 m a.s.l.; green dot in Figure 4), and along the northeastern slope of Gran Sasso Massif at Rifugio Franchetti (2433 m a.s.l.; light blue dot in Figure 4). The northern exposure of these gauges provides a good representation of the climatic conditions occurring in correspondence with the detachment areas of snow avalanches, despite the lack in the snow datasets. Concerning the Rifugio Franchetti gauge, the available data covered different time records (1998–2003 and 2016–2018).

3.4. Nivological Analysis

The local nivological analysis was based on a detailed dataset manually collected at the nivo-meteorological station of the Meteomont service (https://www.sian.it/infoMeteo, accessed on 15 February 2021). It is located at the base of the slope in the Prati di Tivo area (Figure 3), at an elevation of 1450 m a.s.l. It features a northern exposure similar to avalanche-prone regions located at higher elevations. The available historical data for this station begins from the 1977/1978 winter season (from November to April) for 32 surveying seasons. The series is nearly uninterrupted, with a few gaps mostly occurring in correspondence of the beginning/end of seasons. However, data related to the 1992/1994 seasons are completely missing. More in detail, the considered dataset shows several temporal gaps, since it is deeply affected by the irregularity in the opening/closing dates of ski facilities—the former occurring after the first significant snowfall events and the latter during the spring period, usually in the presence of a thick snow cover. This condition was widely relevant before the 1986/1987 winter season and after the 2008/2009 one; consequently, the amounts of seasonal new snow were not correctly computed in these temporal intervals. To reduce this underestimation, we tried to derive good-quality data about the potential snowfall events by computing thermo–pluviometric records at gauges located at a comparable elevation not far from the Prati di Tivo area (e.g., Campotosto gauge, 1344 m a.s.l.—yellow dot in Figure 4). Nevertheless, to deduce a general nivometric trend and better define the nivometric regime of the study area, data belonging to a 20-year time period (1986/1987–2008/2009) were considered and thoroughly analyzed.

3.5. Snow Avalanche Hazard Assessment

This analysis was performed following a stepwise methodological approach that involved the snow avalanche inventory analysis, the analysis and mapping of snow avalanches' paths, the elaboration of a snow avalanche hazard map, and the definition of numerical models.

The snow avalanche inventory was retrieved from the State Forestry Corps of Italy and the Abruzzo Region (http://opendata.regione.abruzzo.it/content/carta-storica-della-valanghe, accessed on 15 May 2021) and allowed us to clearly describe the avalanches' spatial distribution over the study area. Moreover, it was integrated with information derived from the available literature and technical reports [44,75,99].

The analysis of snow avalanches' paths was achieved by combining the literature data, specific site investigations, investigations of the snow-covered ground, interviews of witnesses to past avalanche events, and studying of previous events recorded in various historical and technical archives [44,100].

The evaluation of the snow avalanche hazard map was carried out according to the Swiss mapping criteria [101,102] and thematic guidelines provided by AINEVA (Italian Interregional Association for Snow and Avalanche) [31,103]. Avalanche-exposed zones were defined and annexed within the Avalanche Hazard Exposure Zones Plan—PZEV (Piano delle Zone Esposte a Valanghe in Italian). Generally, this evaluation is fixed through mathematical parameters, which quantified the velocity and flow height, transmitted pressures, and stopping distances of the avalanches [31,102,104,105]. In the invasion zones, as reported in Table 1, some areas are identified and marked with different colors according

to the estimated avalanche hazard—i.e., high hazard with red, moderate hazard with blue, and low hazard with yellow. Town planning and land use prescriptions are fixed for each of the identified zones.

Table 1. Synthesis of the AINEVA criteria [31] for the delimitation and the use of areas with different degrees of exposure to avalanche hazards (T = return time of the avalanche (years) and P_{imp} = impact pressure (kPa)).

Zone/Hazard Degree	Definition Land Use Restrictions
RED High Hazard	Areas affected either by avalanches with T = 30, even with low destructive power ($P_{imp} \geq 3$), or by highly destructive avalanches ($P_{imp} > 15$) with T = 100. New constructions are not allowed.
BLUE Moderate Hazard	Areas affected either by avalanches with T = 30 with low destructive power ($P_{imp} < 3$) or areas affected by rare events (T = 100) with a moderate destructive power ($3 < P_{imp} < 15$). New constructions are allowed but with strong restrictions (low building indexes, reinforced structures, etc.).
YELLOW Low Hazard	Areas affected either by events with a low destructive power ($P_{imp} < 3$) and T = 100 or by events with $100 < T < 300$. New constructions are allowed, with minor restrictions (no public facilities, like schools, hotels, etc.).

In the PZEV's framework, morphometric and nivometric data are generally combined to define the degree of exposure of a specific area in terms of the frequency and intensity of avalanche events. This detailed analysis is usually expressed through:

- the avalanche return period—the average number of years between two events of the same intensity;
- the avalanche pressure—the forces per unit of surface exercised by the avalanche on a flat obstacle of big dimensions disposed perpendicularly to the trajectory of the advancing mass of snow. The pressure can be determined with reference to both the dynamic and static components of the solicitation.

The obtained maps effectively identify the avalanche sites and their expansion in the accumulation zones. This has proven to be most helpful in defining these zones in terms of avalanche frequency and dynamic pressure, thus determining the magnitude/frequency distribution in the runout zones [106–108].

The criteria established and reported in the Avalanche Artificial Detachment Intervention Plan—PIDAV (Piano di Intervento di Distacco Artificiale di Valanghe in Italian) [109] were followed to develop prevention and management activities in the study area. Generally, the main objective of these protection measures is to minimize negative consequences due to snow avalanche risk for people and goods in their settlements and along traffic lines, as well as for skiers [32,110]. The PIDAV plan is a tool, eventually complementary to the aforementioned PZEV, which refers to an area open to the public, clearly defined in space and time, where an artificial release of unstable snow masses is performed to reduce avalanche hazards and risks [109,111]. In case of an urban zone or a ski facility to be protected, as in the study area, it is necessary to define a management measures plan to protect the ski lift. It should include the plan for meteo-nivological conditions monitoring—which are in constant evolution during climatic events—and describes activities to be exerted to learn about this evolution at the meso- and microscale to evaluate snow cover stability conditions and their potential evolution.

In conclusion, this stepwise sequence was completed by avalanche simulation models. In detail, 1- and 2-dimensional avalanche simulation models (e.g., AVAL-1D and RAMMS [39,112]) were applied both to back-analyze documented avalanche events at a particular site, as well as to estimate the consequences of possible hazard scenarios. According to the literature and technical data [102,111,113], the main nivometric parameters required for dynamic avalanche modeling are represented by the maximum height of the

snow cover (Hs) and the increase of the snow cover height over three consecutive days (Dh3gg). For developing the present study, an increase of 5 cm of new snow and a snow cover for every 100 m of elevation was proposed, taking into account the aforementioned literature data and the nivological expert judgment. These physical–mechanical characteristics, together with ancillary information concerning the physiography, steepness, and roughness of the ground, the presence of infrastructures s.l. were reported on a 5-m grid DTM base map and elaborated in a GIS environment.

AVAL-1D is a numerical avalanche dynamics program developed by the Swiss Federal Institute for Snow and Avalanche Research [112]. It allows the simulation of avalanches in one dimension from the starting zone to the runout one. It reproduces runout distances, flow velocities, and impact pressures of both flowing and powder snow avalanches along a specified avalanche track. It consists of two modules: FL-1D (dense flow model) for dense flow avalanches and SL-1D (powder snow model) for powder snow avalanches. It cannot reproduce the whole set of dynamical parameters, since it is a one-dimensional formulation that combines the internal distribution of flowing variables into basic ones controlled by two frictional parameters [114]. In order to supply this not accurately modeling, the RAMMS (RAapid Mass MovementS) code [115] was mainly used to calculate the pressure values on a site-specific avalanche path (such as Vallone della Giumenta) from initiation to runout in a three-dimensional terrain. It is a practical tool for avalanche practitioners, which requires a complete procedure to fulfill the morphological features and release parameters. Moreover, it can be used to estimate runout distances, flow velocities, flow heights, and impact forces [116–118].

4. Results

4.1. Morphometric Analysis

The study area reaches its maximum altitude on the peak of Corno Piccolo (2655 m a.s.l.) and is characterized by a morphology that gradually slopes down to a minimum of 1030 m a.s.l. in correspondence with Pietracamela Village. Based on the orography of the landscape, the area can be fairly divided into three different sectors: a northern one near Pietracamela village, a central one comprising the Prati di Tivo area, and a southern one corresponding to the northern slope of the Corno Piccolo ridge (Figure 5). The northern sector presents the lowest elevation, ranging approximately from 1100 to 1300 m a.s.l.; the slope values range from 0 to 40°, with the maximum values detected in correspondence with the N–S-oriented and, secondarily, W–E-oriented drainage lines; the energy of the relief ranges from 250 to 350 m, with the highest values along the Rio San Giacomo. The central sector is characterized by a flat and irregular morphology, featuring elevations ranging from 1300 to 1700 m a.s.l., and a homogeneous slope distribution (values between 5° and 20°); the energy of the relief, on the other side, shows heterogeneous values ranging from 250 m towards the western portion to 400 m towards the eastern one. The southern sector, finally, presents elevations ranging from 1700 up to 2500 m a.s.l.; the slope distribution is dominated by the highest values (between 60° and 80°), with peaks detected in correspondence with the N–S-oriented drainage lines and W–E-oriented steep scarps; the energy of the relief ranges from 500 up to 600 m, with the highest values along the northern escarpment of Corno Piccolo.

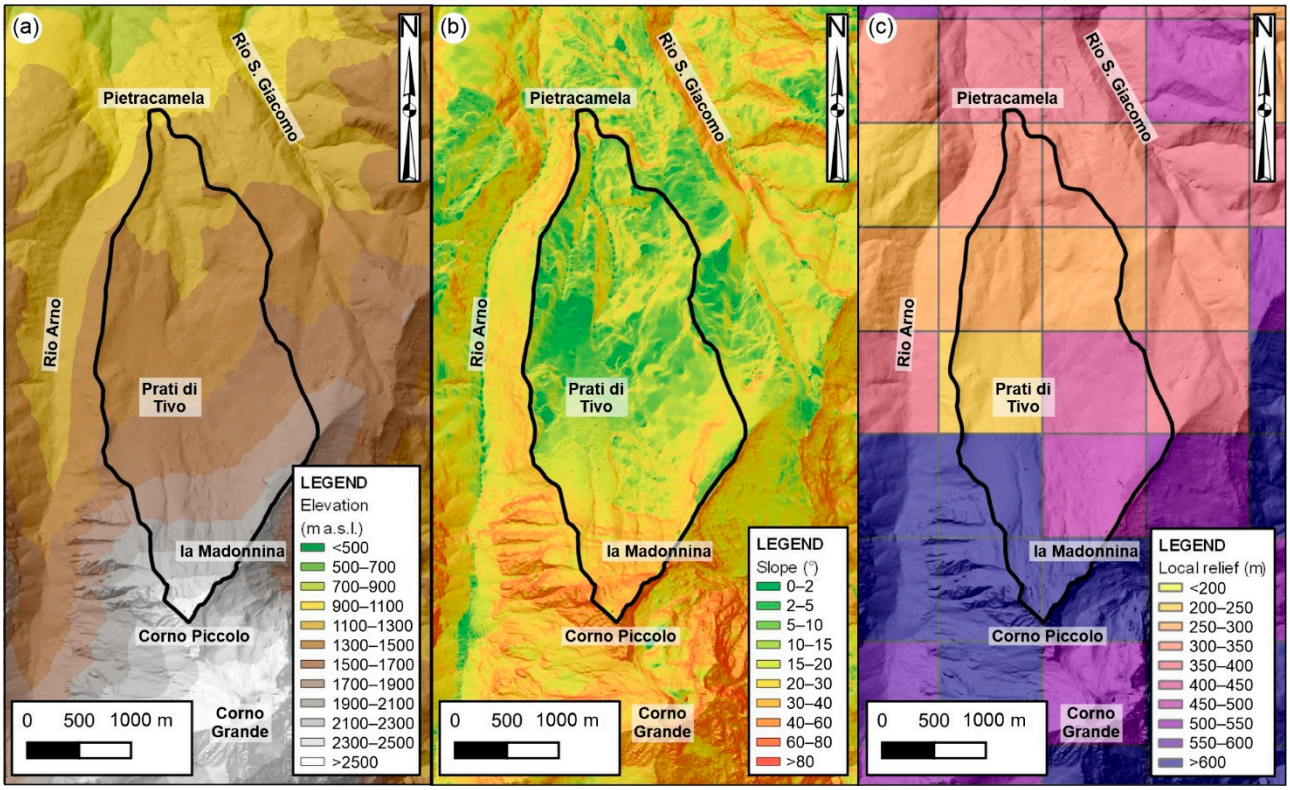

Figure 5. Physiographic features of the study area: (**a**) elevation map, (**b**) slope map, and (**c**) local relief map. The black line represents the study area.

4.2. Geomorphological Analysis

The study area is characterized by the outcropping of lithological sequences belonging to pre- to sin-orogenic deposits. In detail, it is characterized by calcareous and marly deposits outcropping in the southernmost sector, in correspondence with the Corno Piccolo ridge. Instead, the central sector is dominated by the presence of arenaceous-pelitic and pelitic-arenaceous deposits, mainly composed of turbiditic layers with fine sand or coarse silt and pelitic intercalations. The bedrock is widely covered by continental deposits (Figure 6). Scree slope deposits, mainly composed of cemented breccias, characterize the westernmost sector and, locally, the easternmost one, near la Madonnina.

In the Prati di Tivo area, recent glacial and alluvial fan deposits are present along the N–S-elongated outcrops; moving eastward, fluvio-glacial deposits, consisting of cemented breccias and largely marked by landslide bodies, alternate with recent scree slope deposits.

From a geomorphological standpoint, the most recurrent features are represented by structural, slope, fluvial, and glacial landforms (Figure 6). Concerning structural ones, in the southernmost sector, a W–E-oriented is detectable, overlapping calcareous deposits on overturned marly deposits. A second buried thrust is not clearly observable, but its existence can be inferred through minor in-field exposures that highlight the overlapping of marly deposits over sin-orogenic pelitic-arenaceous deposits. Slope landforms partly consist of active rockfalls and complex landslides in the northern sector near Pietracamela.

Large quiescent rotational and translational slides affect the central-eastern portion of the study area east of the Prati di Tivo area, together with localized quiescent earthflows. Smaller rotational and translational slides are found towards the north, mainly set on pelitic-arenaceous deposits. Finally, N–S-oriented rock gullies with debris discharges characterize the northern slop of the Corno Piccolo ridge. Landforms due to running water are mainly represented by a wide alluvial fan, as well as of several gullies; both are present in the western part of the study area, within the Prati di Tivo area, the former being set between glacial (to the West) and landslide (to the East) deposits, the latter with

a general N–S direction and extending along the main drainage line. Finally, concerning glacial landforms, several scarps are preserved as relict landforms in the southern sector. Furthermore, several N–S-oriented avalanche tracks characterize the norther escarpment of the Corno Piccolo ridge, alternating themselves with the rock gullies.

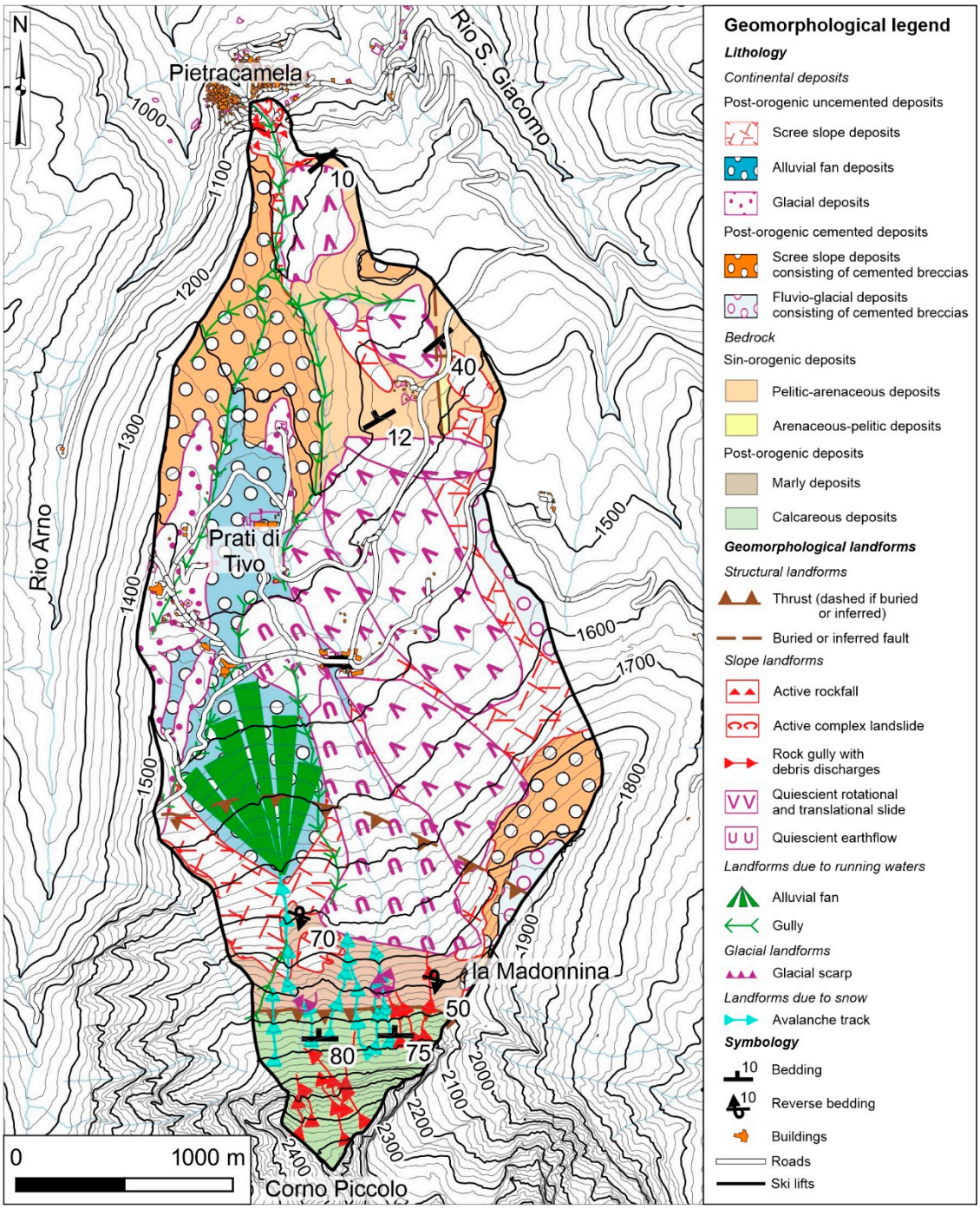

Figure 6. Simplified geomorphological map of the study area (modified and updated from [65,88,89]). The black line represents the study area.

4.3. Climatic Analysis

The microclimatic features of the study area were analyzed considering the historical thermo–pluviometric series available at the Pietracamela gauge (1043 m a.s.l.), covering a 50-year time period (1951–2004); nevertheless, the selected gauge is located approximately

400 m below the Prati di Tivo area and at least 1000 m downstream of the main avalanches and landslides detachment areas (Table 2). Nonetheless, for the study area, it was impossible to define spatial and altitudinal meteoric features since snowfall and rainfall events are often coupled with strong winds that can induce relevant rates of underestimations, especially at the highest elevations.

Table 2. Main values of the temperature and rainfall, resulting from the climatic analysis at the Pietracamela gauge (1043 m a.s.l.).

Yearly Average (1951–2004)		**Monthly Average (1951–2004)**												
Temperature (°C)			Temperature (°C)											
			Jan	Feb	Mar	Apr	May	Jun	Jul	Aug	Sep	Oct	Nov	Dec
Frost days	65	Frost days	16	15	12	4	0	0	0	0	0	1	5	12
Absolute maximum	36.8	Absolute maximum	19	20.7	25	24.5	31.5	35	35	36.8	34	27.8	25	22
Daily average	10.7	Daily average	3	3.4	5.5	8.4	12.8	16.7	19.7	19.8	16	11.3	7.2	4.2
Mean maximum	14.6	Mean maximum	6.5	7.2	9.4	12.4	17	21.2	24.5	24.6	20.2	14.9	10.4	7.4
Mean minimum	6.7	Mean minimum	−0.4	−0.5	1.5	4.4	8.7	12.3	14.9	14.9	11.8	7.7	4	1.1
Absolute minimum	−14	Absolute minimum	−14	−12.8	−12.1	−7	−0.5	3	4.5	4	−1.3	−7	−7	−13
Rainfall (mm)														
Total rainfall	1065.3													
Maximum in 1 h	57.8		Jan	Feb	Mar	Apr	May	Jun	Jul	Aug	Sep	Oct	Nov	Dec
Maximum in 24 h	268.6	Total rainfall	85.4	74.8	95.7	110.4	82.5	68.1	44.9	51.8	78.3	117.1	136.3	120.0
Rainy days	106	Rainy days	8.5	9.1	9.7	10.6	10.0	8.0	6.2	5.8	7.2	9.8	10.8	10.6

The average annual temperature is ~10.7 °C, with an average daily thermal excursion of ~7 °C; the maximum temperatures can eventually exceed 35 °C, while the minimum ones almost reach −15 °C. Frost days (T_{min} < 0 °C) are ~65 per year, while ice days (T_{max} < 0 °C) are no more than 10 per year.

The total rainfall is moderately abundant with respect to the Gran Sasso Massif geographic location, exposed to "Tramontana" and "Bora" dry and cold winds, as well as to "Scirocco" and "Libeccio" wetter ones, which often release the moisture taken in charge. During the summer, the ascent of convective cells from the near L'Aquila Basin and the middle Vomano River valley is common. The total annual rainfall is approximately 1100 mm, distributed along with an average of 106 rainy days; the hourly and daily maximum values, respectively, correspond to 58 mm and 267 mm. The meteoric regime shows peculiar features pertaining to the Apennine–Adriatic type [81,100], with a bimodal rainfall distribution characterized by a global maximum value in November with a secondary peak in April and a global minimum in July/August—months not in a drought, given the frequent occurrence of convective phenomena—with a secondary peak in February. It should also be stressed that the monthly rainfalls never drop below 50 mm.

Snowfalls are frequent during every winter season, with high amounts with respect to the geographic position of the study area, as previously reported in the thematic literature [100,119]. Considering the possible influence of disturbing fluxes coming from the south and associated with negative temperatures, the study area can present cumulative values among the highest of the Central Apennine area, as happened in February 2017 [119].

The performed climatic analysis confirms, even in this area, an increase of the temperature values of about 1.1 °C during the last 50 years; unfortunately, the weather station located at Pietracamela ceased its activity in 2004, thus making a more recent trend analysis impossible. The rainfall regimes, on the other side, do not show significant variations (−1.5 mm/year), but it is possible to observe a decrease of about 10% in the number of days with precipitation rates > 1 mm from 110 to 101; consequently, the average daily rainfall

intensities have slightly increased. Considering the recorded datasets, homogeneous and complete data relating to short and intense precipitation events is unavailable. It was not possible to perform a comprehensive analysis for this specific climatic aspect.

The detailed climatic analysis shows that average annual temperatures for the year 2020, as observed for the Teramo gauge (blue line in Figure 7a), was approximately 1 °C higher than the conventional 30-year time period (1971–2000), known as CliNo (Climate Normal). Consequently, the elevations of the 0 and −1 °C isotherms correspond to 3099 and 3296 m a.s.l., far above those calculated by Dramis et al. [120], corresponding, respectively, to 2615 and 3028 m a.s.l. Considering that the average annual temperature recorded at the Pietracamela (1043 m a.s.l.) and Rifugio Franchetti (2433 m a.s.l.; green line in Figure 7a) gauges are, respectively, 10.7 and 2.6 °C, given a difference in elevation of about 1500 m, a vertical thermal gradient of approximately 6.1 °C/km can be estimated. Thus, an average annual temperature of 7.6 °C and 4.2 °C can be derived at, respectively, Prati di Tivo (orange line in Figure 7a) and the avalanche detachment areas located at ~2200 m a.s.l.

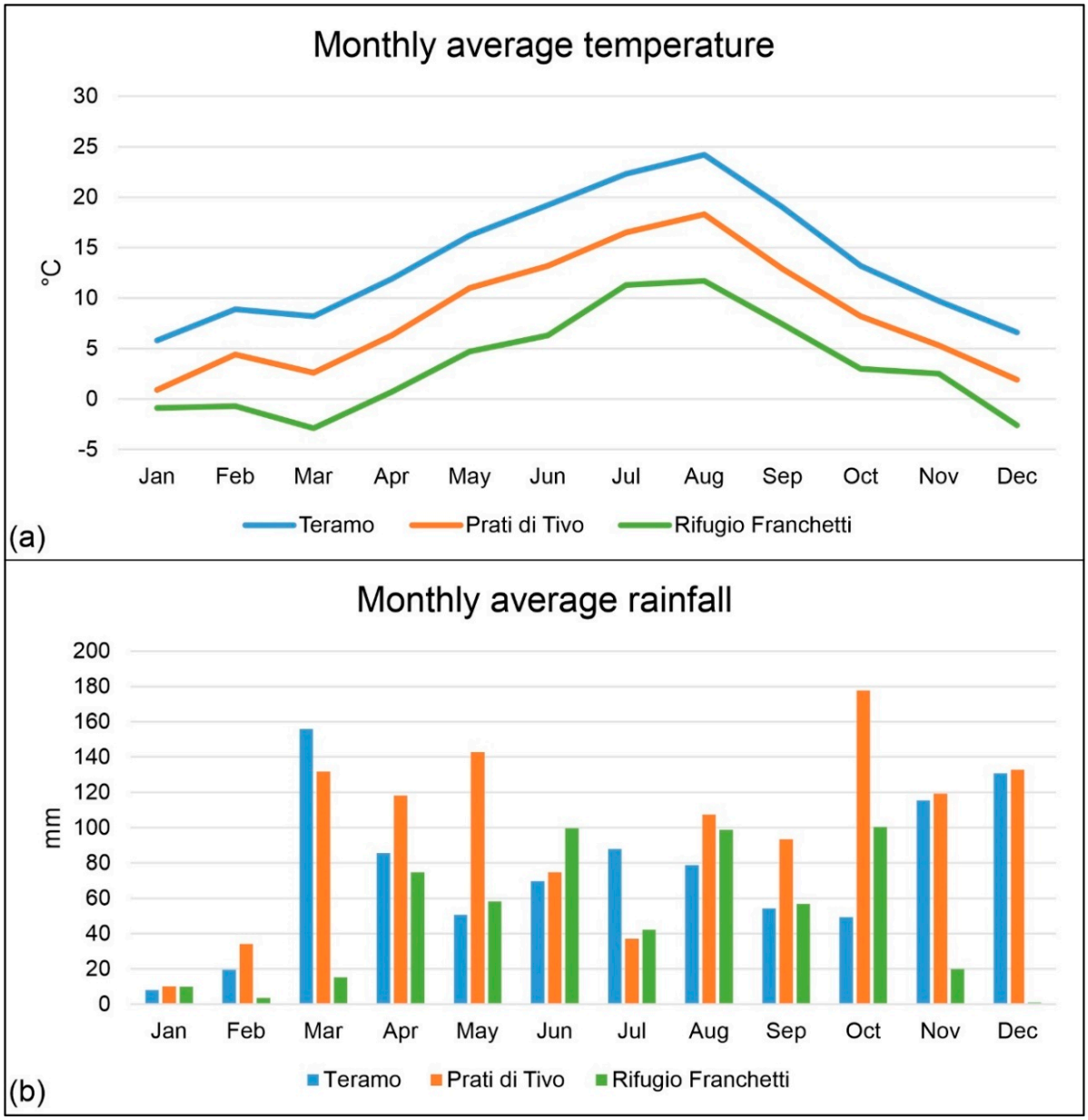

Figure 7. Monthly average temperature (**a**) and monthly average rainfall (**b**) trends for the year 2020.

The monthly average rainfalls (Figure 7b) show a noticeable growth with a direct relationship as the altitude increases due to an orographic effect, in accordance with previous estimates made for this sector of the Central Apennine Chain (30 mm/100 m) [100,119]. Nevertheless, a drastic decrease of these values occurs at higher elevations, which is typical of an arid boreal habitat. This substantial underestimation, up to 70%, occurs in areas exposed to powerful winds during rainfall and/or snowfall events [121].

The anemometric signal is significant in the whole area from 260 up to 2400 m a.s.l., thus promoting the accumulation of frames and lenses above all on the ridges of Gran Sasso Massif and in correspondence of steep channels and depressed morphologies downwind of the main flow during and after snowfalls (Figure 8a). In particular, at high elevations, the number of days with a maximum wind speed greater than 30 km/h, sufficient for inducing a reworking of the snow cover, is around 40. Main winds come from the second and the third quadrants during the winter, reaching speeds greater than 200 km/h (Figure 8b).

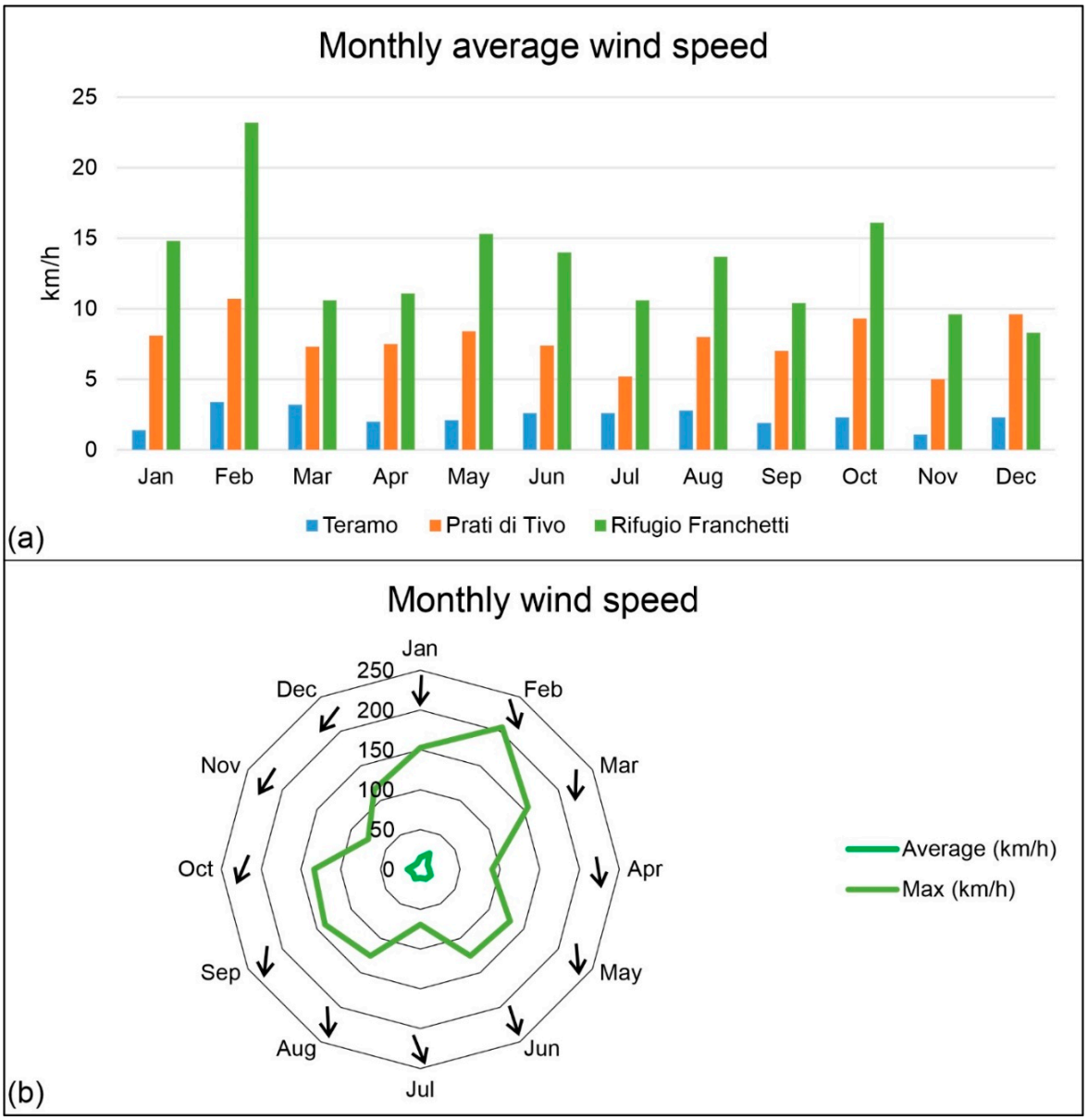

Figure 8. (**a**) Monthly average wind speed for the year 2020 and (**b**) monthly wind speed recorded at Rifugio Franchetti (2433 m a.s.l.). Black arrows indicate the monthly average direction of winds.

4.4. Nivological Analysis

By accounting for limits derived from the available nivological data, as previously reported in the Materials and Methods section, the following can be stated:

- The Prati di Tivo area shows a regular snow cover every year relatively abundant in certain winter seasons, such as 1994/1995, 1998/1999, and 2004/2005, with cumulative values greater than 400 cm. Only during the 1988/1989 winter season, the cumulative was less than 100 cm (Figure 9a). Recently, a more significant snowfall irregularity occurred, with long phases characterized by the absence of snow phenomena, alternating with short but intense heavy snowfalls events. Accumulations seem to have increased against a lower persistence of the snow cover. The trend analysis referring to the aforementioned period depicts a clear rise in the signal—over 3 cm per winter season—deriving from the highly irregular nivometric trend, with a hint of a ten years of periodicity and a more recent signal of about 3.8 cm per winter season detected on average for the Central Appennines Chain [100,119,122].
- Heavy snowfalls already occur from the middle of November. They are common throughout the winter and until the second half of March, becoming sporadic in April (Figure 9b). By accounting for the available datasets, the absolute monthly maximum values occurred in January 2017 at about 425 cm distributed in only seven days [119]. The winter's least snowy month is estimated to be December. The snowfall regime (Figure 8b) presents a unimodal distribution, with the maximum values detected in January and February. Arguably, for altitudes greater than 2000 m a.s.l., the trend tends to become fairly regular if not bimodal with a second peak during the spring, given the notable snowfall increase in March and April, as detected at the Campo Imperatore gauge (2137 m a.s.l.).
- The number of snowy days shows considerable intra-seasonal variations, strictly dependent on the synoptic seasonal evolution. This aspect was particularly evident in the last decade, albeit in a context of significant snowiness, with values ranging between 25 and 35 events per season, with peaks of about 40. During the last seasons, a general decrease of the phenomenology seemed to be occurring; these are increasingly concentrated in a few days and present a greater intensity, which underlines the climatic extremization in progress. Furthermore, a delay at the beginning of the snowy season seems evident, along with a greater frequency of events at the beginning of the spring season.
- Daily snowfall data (Figure 10a) highlight the possible occurrence of snowy events of high intensity and short-to-moderate durations. In particular, the maximum recorded daily amount of fresh snow is around 70 cm (13 February 1986 and 23 March 2009). Moreover, it is essential to consider unofficial recordings performed on 17–19 January 2017 (when abundant avalanche events occurred, reaching the Prati di Tivo area and causing considerable damages to infrastructures and ski facilities), which pointed out a daily maximum of 140 cm on 17 January and of 310 cm for the whole three-day period.
- Significant sudden temperature changes occurring more frequently after or during snowfalls generally disfavor the cohesion process between the strata composing the snow cover, thus causing a hypothetical increase of the avalanche hazard. Nevertheless, a clear Mediterranean type, the climatic extremization, and a not-excessively-high elevation determine an early beginning of the accelerated destructive metamorphism processes, with a subsequent quick decrease of the snow depth values on the ground up to the maximum elevation of avalanche-prone areas. Furthermore, close to detachments areas, a strong wind power occurring during and after snowfalls induces rapid mechanical metamorphism. In the case of intense snow events followed by exceptionally cold climatic phases and variable weather conditions, destructive metamorphism processes take place very slowly; constructive metamorphism is indeed established. The thickness of the snow cover remains relatively abundant for a long time (Figure 10b).

- Days with mixed snowfall and rainfall events or entirely rainy ones are also estimated to occur during the winter season. This is connected to the synoptic conditions inducing rainfall and to the eventual mixing within the frontal system. Field evidence and surveys in specific sites suggest that this has a significant repercussion on natural avalanche occurrences, especially below 1900 m a.s.l.
- From field surveys, as well as from the avalanche inventory and literature data (i.e., Meteomont service), it results that, in correspondence with a sudden temperature rise, avalanche events may occur with loose surface cohesion values already in the 24–36 h following the snowfall events, involving many buildings and anthropic structures present in the Prati di Tivo area.

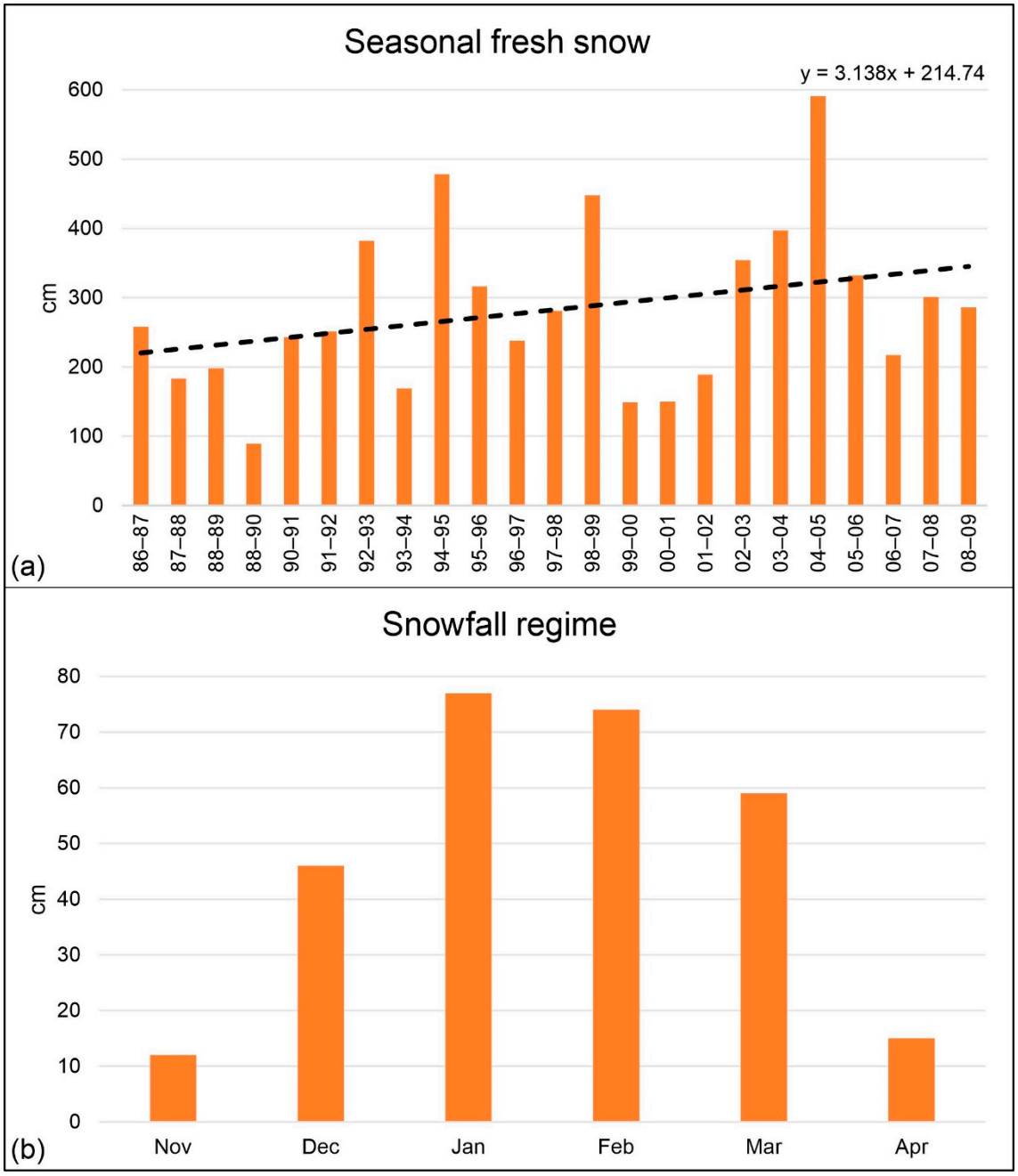

Figure 9. Seasonal fresh snow trend for the timespan 1986–2009 (**a**) and snowfall regime (**b**) at the Prati di Tivo gauge (1450 m a.s.l.).

In order to provide a complete and updated description of the nivometric trends, the historical series and datasets available at the Rifugio Il Ceppo gauge (1340 m a.s.l.) were analyzed. This weather station was taken into account since it shows snowmaking very similar to that of Prati di Tivo, even if it is located on the eastern side of the neighboring Laga Mountains at a distance of about 20 km from the study area.

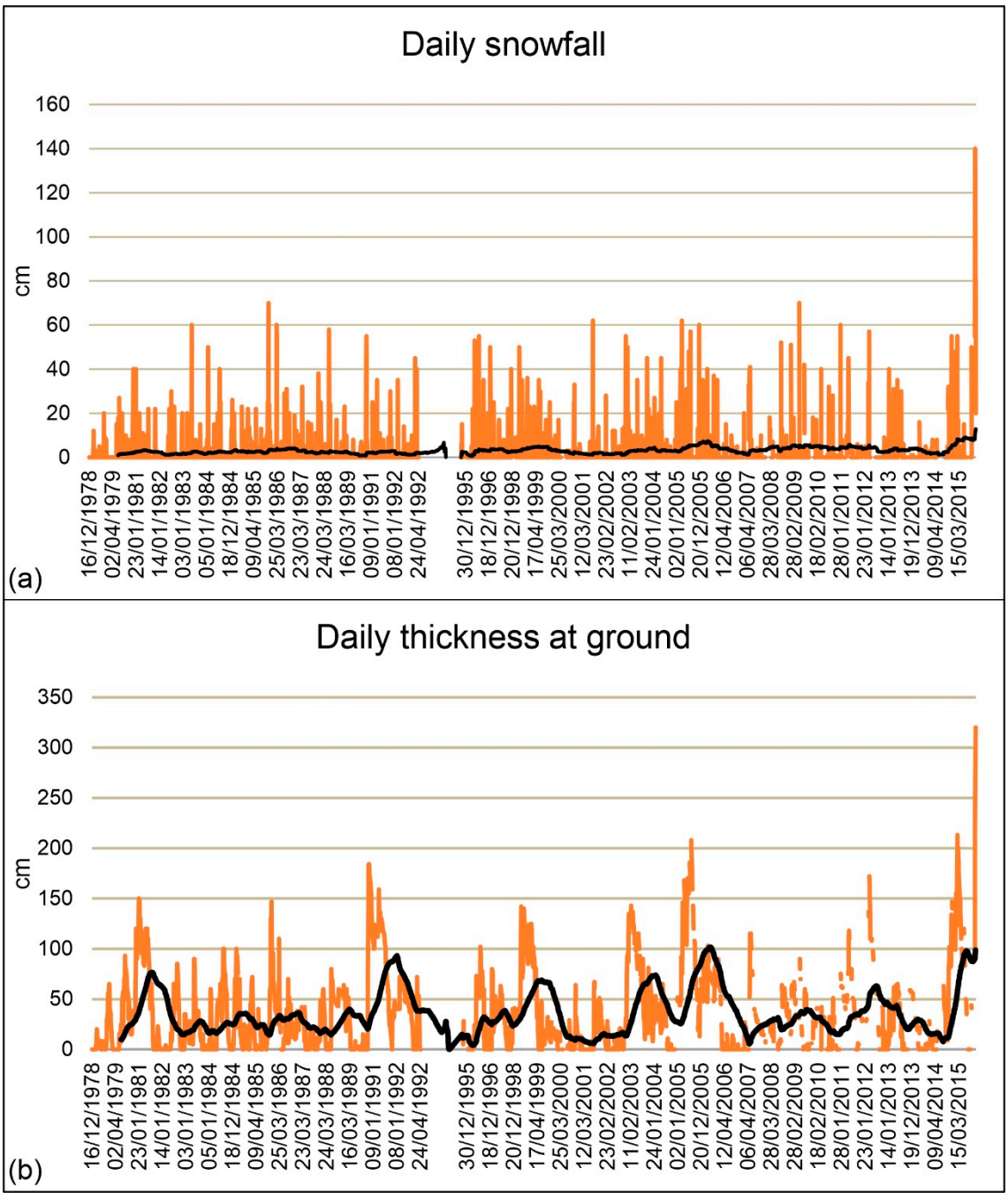

Figure 10. Daily snowfall (**a**) and snow cover thickness (**b**) at the Prati di Tivo gauge (1450 m a.s.l.).

As graphically reported in Figure 11, the nivometric trend spanning over a 40-year time period (1979–2019) confirms the increase of snow precipitation. However, it is less marked than that evident for the Prati di Tivo area (Figure 8a), with a minimal difference in the recent interseasonal variations (2.1 cm vs. 3.1 cm/season), whose trends are increasingly marked.

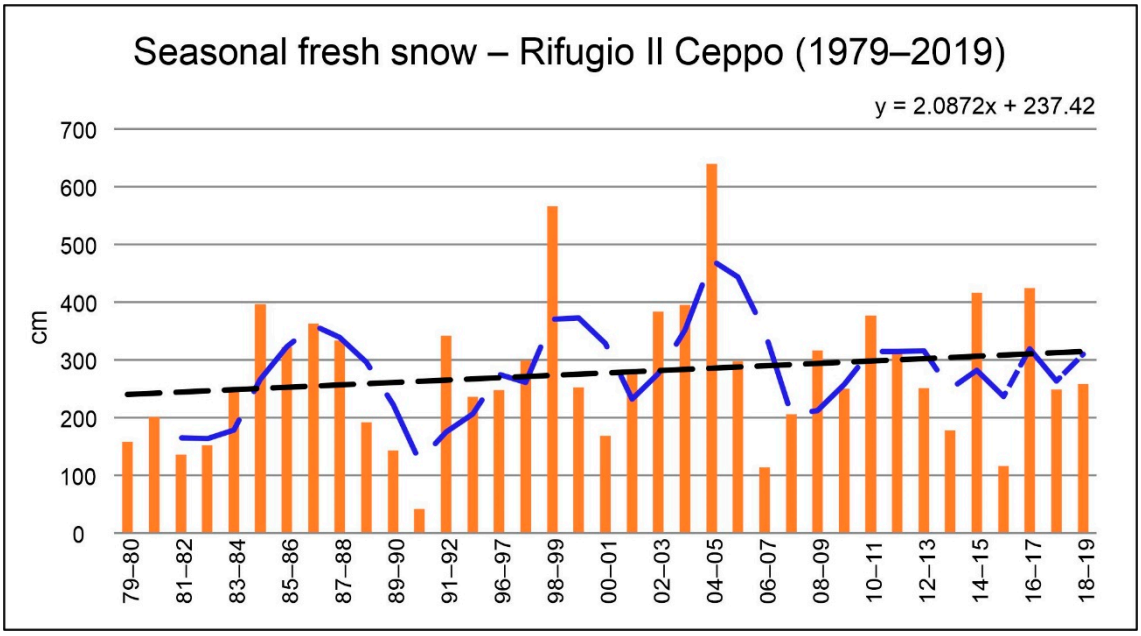

Figure 11. Seasonal fresh snow at Rifugio Il Ceppo (1340 m a.s.l.). The blue dashed line represents the 5-year moving average.

4.5. Snow Avalanche Hazard Assessment

A stepwise methodological approach allowed us to perform a complete snow avalanche hazard assessment, also taking into account the study area's main physiographic and geomorphological features. The avalanche-prone areas along the main N–S-oriented avalanche tracks characterize the northern escarpment of the Corno Piccolo ridge, which alternate with several rock gullies. The area shows elevation values ranging from 1320 to 2270 m a.s.l. As confirmed by the previous data and analysis [123,124], the avalanche paths largely affected residential structures and ski facilities, causing significant damages in recent times.

Firstly, a snow avalanche inventory analysis was carried out. The geodatabase retrieved from the State Forestry Corps of Italy and the Abruzzo Region stored and collected almost 800 avalanches over the whole Abruzzo Region from 1957 to 2013. The yearly number ranged up to 70 in the last decades, and about 40 events were recorded in the previous years covered by the catalog, with a poor direct correlation with the snow thickness. As graphically reported in Figure 12, for the Prati di Tivo area, the database reports 131 snow avalanches: 10 of which accounted as slab snow avalanches, 26 as glide snow avalanches, 54 as powder snow avalanches, 9 as loose snow avalanches, and 32 as mixed or not classified snow avalanche.

Additionally accounting for the main geomorphological features, a preliminary analysis of the spatial distribution of snow avalanches over the study area shows the northern escarpment of the Corno Piccolo ridge almost totally affected by avalanche phenomena whose detachment areas are located at elevations ranging from 1700 up to 2550 m a.s.l. These phenomena mainly involved several N–S-oriented rock gullies and trails, often anastomosed, allowing the snow movements to extend heterogeneously, depending on the type and amount of snow involved.

Moreover, to provide a complete inventory, official avalanche data of the Abruzzo Region were integrated with the literature data, local chronicles, eyewitness reports of past avalanche events, and studies of previous events recorded in various historical and technical archives.

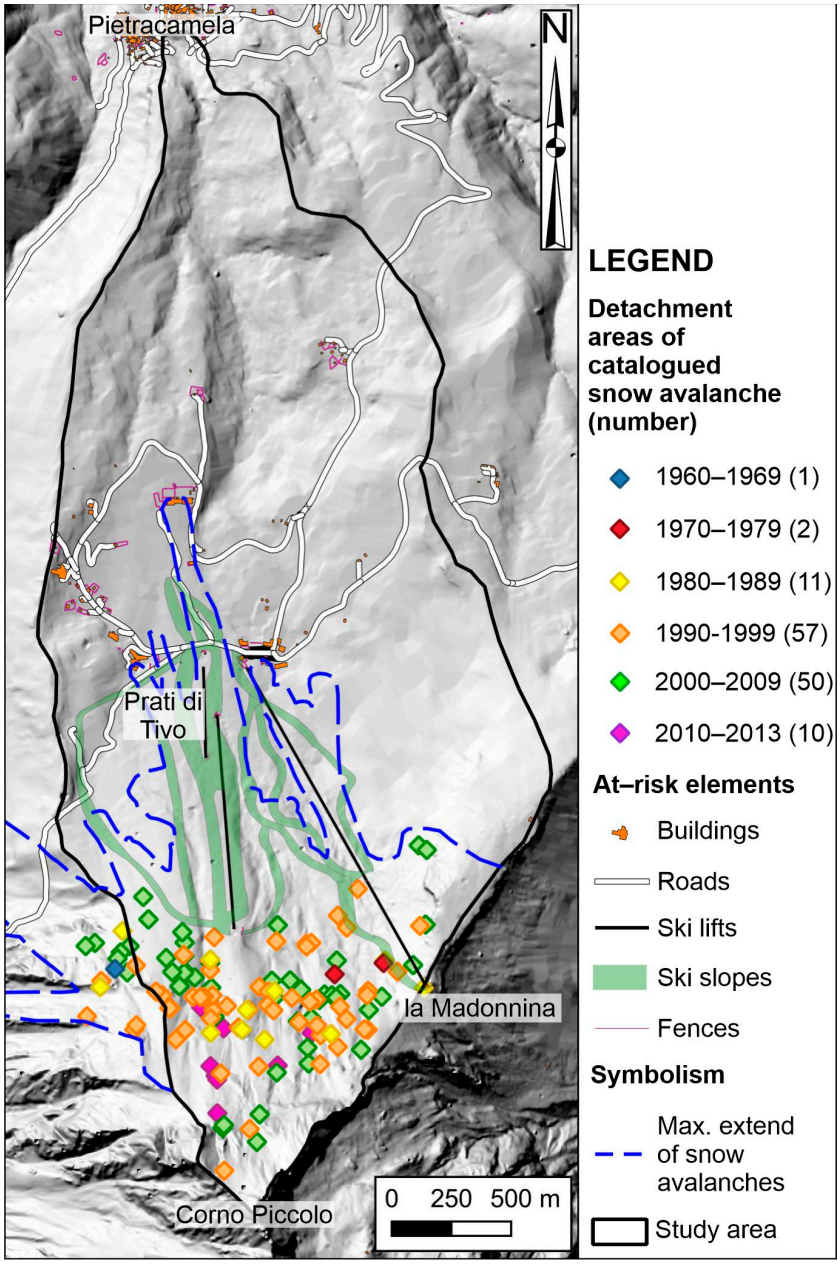

Figure 12. Historical snow avalanche map of the study area (1957–2013 period).

The study area has suffered a rapid and intense urban development for sport tourism purposes since 1965, although several avalanches have occurred in the past, according to local chronicles and eyewitness reports. These events were also integrated into the snow avalanche inventory analysis, enabling the mapping of the maximum extent of avalanches in the Prati di Tivo area. They are chronologically reported as follows:

- April 1929 (not reported in the official database of Abruzzo Region)—A large avalanche event reached the Guide Shelter (Rifugio delle Guide in Italian).
- 7 April 1978—A large avalanche, detached from the northern escarpment of the Corno Piccolo ridge, moved down through rock gullies and affected the ski lift and the other facilities downstream to the Madonnina location.
- 8 January 1981—An avalanche, detached from the northern slopes of the Corno Piccolo ridge, affected some houses and buildings located at Prati di Tivo.
- 2 March 1984—An avalanche affected the study area and posed in a threat the Madonnina chairlift bar.

- 3 March 1999—A large avalanche hit the study area, causing several damages to the ski facilities (e.g., pylons, intermediate station, and ticket office).

The resulting data highlight a scarce spatial characterization of snow avalanches along the study area. Given the proximity of different detachments sites, the reconstruction of past avalanche activity remains quite difficult, distinguishing events occurring from neighboring detachment areas. Consequently, considering the absence of an updated Probable Avalanche Location Map—CLPV (Carta di Localizzazione Probabile delle Valanghe in Italian) [44], an analysis of snow avalanches' paths was performed to identify areas likely to be exposed to avalanche hazard. This "static" approach [105,125] was based on the analysis of morphological features for delineating the predisposition to snow avalanche occurrence within the whole northern escarpment of the Corno Piccolo Ridge, also considering the spatial distribution and the recurrence of the main phenomena. Six main avalanche paths were selected (Figure 13) that are considered the most likely to occur and affect houses, roads, and sporting infrastructures. Moreover, most of the chosen sites were devoid of terminology, and according to their proximity to isolated buildings or specific sites/localities, it was decided to provide detailed descriptions for some of them.

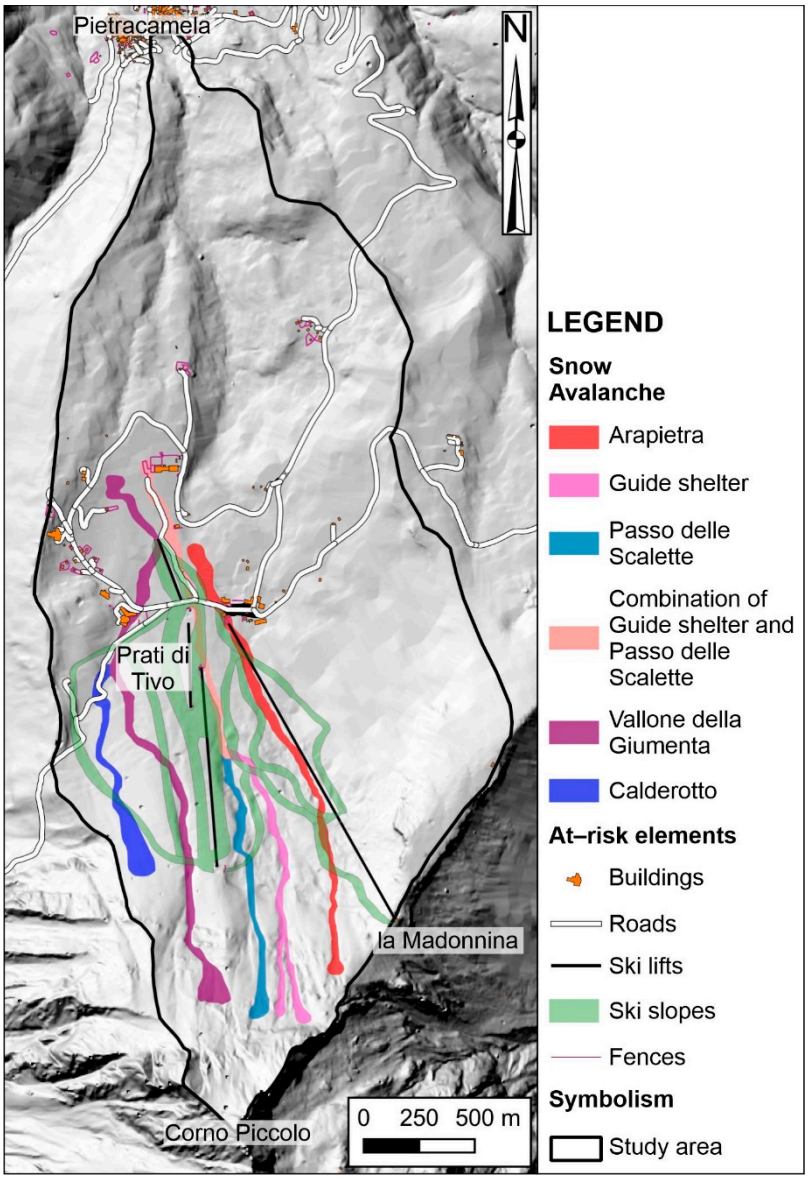

Figure 13. Snow avalanche paths recorded and mapped in the present study.

The exceptional snowfall events generating the snow avalanche disaster involving the Rigopiano Hotel in January 2017 [75,126,127] caused several collateral events in the surrounding areas, including the Prati di Tivo area. They generated a wide snow avalanche along the Vallone della Giumenta (Figure 13) and determined acute injuries to the Prati di Tivo residence (Figure 14).

Figure 14. Detail of damage caused by the Vallone della Giumenta avalanche to the Prati di Tivo residence on 18 January 2017 (source Il Martino, 2017). For the avalanche path's location, see Figure 12.

This event led to the definition and realization of the first Avalanche Hazard Map of the entire Central Appennines area within the Avalanche Hazard Exposure Zones Plan—PZEV (Piano delle Zone Esposte a Valanghe in Italian). At the same time, the PIDAV was presented to develop prevention, mitigation, and management activities of ski facilities directly exposed to avalanche dynamics [100]. In this context, the nivometric dataset available at Prati di Tivo gauge (1450 m a.s.l.) was widely analyzed to derive the required parameters for dynamic snow avalanche modeling (Table 3). This analysis allowed us to define the possible return times of snowfall events at different periods. In detail, the relationship between the maximum height of the snow cover (Hs) and the increase of the snow cover height over three consecutive days (Dh3gg) revealed that snow events (i.e., January 2017) that created a Hs > 3 m can be statistically considered as significant outliers (std > 3) with potential return times far exceeding 300 years.

Table 3. Main nivometric parameters required for the return time estimations, recorded at the Prati di Tivo gauge (1450 m a.s.l.). N.B.: Hs is the height of the snow cover and DH3gg is the increase of the snow cover height over three consecutive days.

					Return Time (Year)					
Hs (t)	**5**	**10**	**15**	**30**	**50**	**100**	**150**	**200**	**300**	**500**
cm	154	177	191	213	229	251	263	272	285	301
					Return Time (Year)					
DH3gg (t)	**5**	**10**	**15**	**30**	**50**	**100**	**150**	**200**	**300**	**500**
cm	64	78	86	99	109	122	130	135	143	153

A thematic map elaborated following the AINEVA criteria [31] and integrated with a detailed nivological analysis is graphically shown in Figure 15. This map clearly shows the main areas exposed to avalanche hazards. Considering the spatial distribution of the snow avalanche paths, as reported in Figure 12, it is possible to delineate the transit and invasion zones, marked with different colors according to the estimated avalanche hazard and the potential return periods (such as T = 30, 100, and 300 years). The analysis of the map highlights different scenarios: with a return time equal to 30 years, all tourist, sporting, and residential facilities can be affected by significant snow avalanche phenomena characterized by paths that reach the Prati di Tivo area at elevations of 1450 m a.s.l., while avalanches with a return time equal to 300 years can get a wider spatial extension (downward to 1370 m.a.s.l.) comparable to the maximum extent of the historical snow avalanches previously described (dashed blue line in Figure 12).

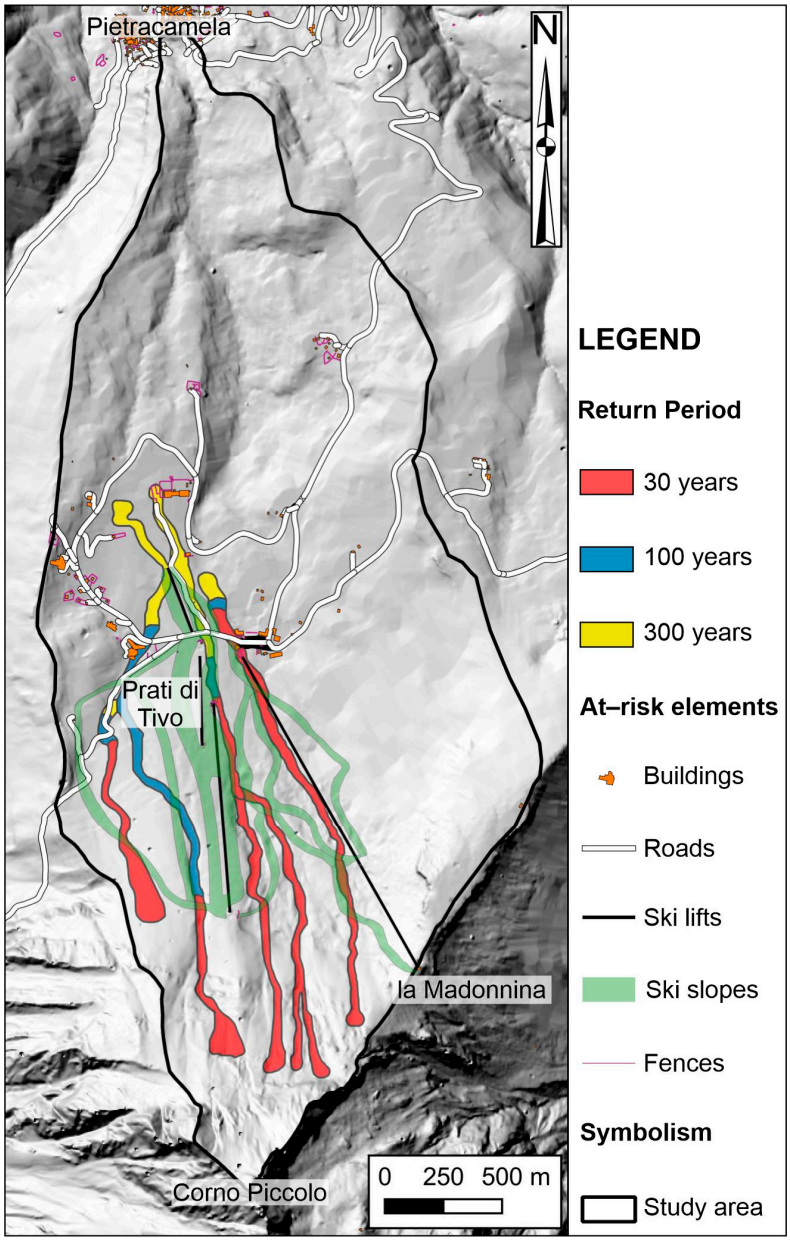

Figure 15. Avalanche hazard map of the Prati di Tivo area. Areas affected by snow avalanches with a return time equal to 30, 100, and 300 years are shown, respectively, in red, blue, and yellow.

5. Discussions

Snow avalanche hazards are computed to be increasing worldwide due to climate changes [128,129]. Among all the climatic contributors, climate extremization is identified as one of the factors influencing the behavior, irregularity, and frequency of snow avalanches [130,131]. In some areas, it causes the thinning and shortening of the duration of snow cover, contributing to an increased irregularity that raises the hazard. As a result, a correct climatic analysis involving investigations of changes in the snow cover and snow avalanche hazard assessment is vital for administering many crucial societal issues concerning territorial planning, risk mitigation, and resilience activities [25,132,133].

Exposure to this hazard may be voluntary, as is the case with skiing, or involuntary, such as on public transportation corridors and settlements. According to the literature and technical reports [31–33], the techniques used to evaluate avalanche hazards and risks are different depending on the circumstances.

Here, we attempted to understand the main interrelationships between climate extremization and environmental risk in a mass movement-prone area, such as the Prati di Tivo area. We discussed the stepwise approach to be followed for a correct snow avalanche assessment by combining the spatial distribution of the snow avalanches and the main climatic features of the study area. It was also essential to compare the findings with the detailed geomorphological features of the Vallone della Giumenta to outline the role of climate extremization in the triggering of the avalanches.

The combination of preliminary results and thematic maps allowed us to better characterize the study area from a morphometric, geomorphological, climatic, and nivological standpoint. In such a complex and mass movement-prone area, it was necessary to activate a risk mitigation protocol to develop land use policies and activities to define a significant snow avalanche assessment. According to the PIDAV project [99], the safety services for ski resorts and facilities at Prati di Tivo were updated by installing 12 Obellx® gas exploders [109,134] to manage short-term avalanche risks better. The installation was realized in correspondence with the main detachment areas at elevations ranging between 2100 and 2250 m a.s.l.

Moreover, as part of the increasingly more frequent processes of climate extremization, on 24–26 March 2020, a heavy snowfall event affected the study area. It was acknowledged as a prevalently stormy snowfall, which brought 90 cm of fresh snow (with a density of 140 kg/m^3) over the ski facilities located at Prati di Tivo at elevations of about 1400 m a.s.l. Given the high snow accumulation rates, explosive pitches were performed on 24 March immediately after the beginning of the snowfall event and on March 26 during the main event, inducing moderate detachments of fresh, humid, and low-cohesion snow. Even if the preventive activity of Obellx® gas exploders reasonably mitigated the snow dynamics, on the night of 27 March, around 4:20 a.m., two natural snow avalanche events occurred following new abundant snowfalls and affected the northern escarpment of the Corno Piccolo ridge (Figure 16). A detailed field survey and a specific site investigation were also performed in the early morning of 28 March, thanks to a clear weather improvement. Considering the information gathered from this survey, it was possible to make several essential deductions:

- Slightly downstream of the prominent peak (Corno Piccolo, 2655 m a.s.l.) at an elevation of about 2550 m a.s.l., a detachment area was visible, as graphically shown in Figure 16a. Moreover, according to no official local chronicles and eyewitness reports, it seemed to correspond with the site of an avalanche never reported and stored in the Geodatabase of the Abruzzo Region.
- The whole avalanche path mainly affected the Vallone della Giumenta (for the site's location, see Figure 13), with a clearly outlined detachment area at an elevation of 2300 m a.s.l. (Figure 16b).
- Significant snow accumulations generated by the snow mass releases produced by the Obellx® devices on the 25th and 26th of March were visible throughout the escarpment.

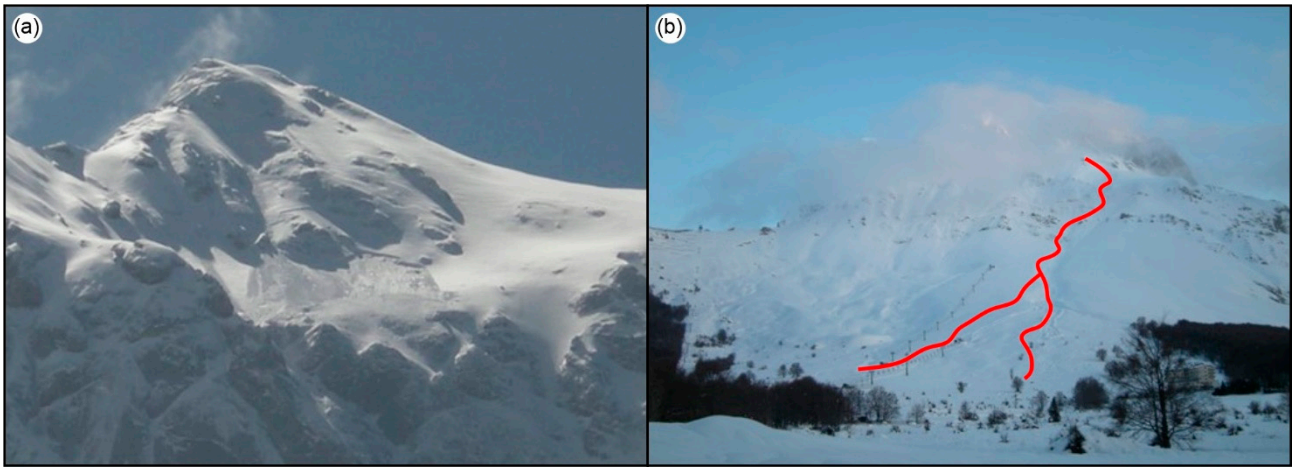

Figure 16. Photo documentation of the snow avalanches of March 2020. (**a**) Evidence of the summit detachment area at the base of Corno Piccolo with a clear surface slab and (**b**) a simplified snow avalanche path (in red) affecting the Vallone della Giumenta and involving the main ski facilities.

The presence of interdigitated snow mass accumulations belonging to the March 2020 avalanches, both partially converged into the Vallone della Giumenta, testified the dynamic avalanche framework of the study area. Unfortunately, this peculiar nivological setting makes it impossible to define the temporal evolution of the two different events. For these reasons, preliminary one- and two-dimensional avalanche simulation models (e.g., AVAL-1D and RAMMS [39,112]) were applied to better describe the possible evolution of the documented avalanche events at a particular site (such as the Vallone della Giumenta), as well as to calculate the consequences of possible hazard scenarios. The avalanche modeling was carried out by employing RAMMS software and implemented with GIS techniques. In detail, it was performed both by considering a scenario characterized by a limited thickness of the snow cover mitigated by the Obellx® devices' activity and a scenario in which the downstream slopes were totally covered by a thick snow cover (i.e., not secured by the preventive action of the Obellx® devices). The resulting data defined different stopping distances and paths of the selected avalanche under scenarios driven by other transmitted pressures, as graphically shown in Figure 16. It showed how, in the absence of the preventive action of the Obellx® devices (red stars in Figure 16), an avalanche event can predominantly occur along the Vallone della Giumenta. Moreover, transmitted pressures, which vary from 30 to 150 kPa, and different heights of snow cover (Hc = 0.5, 1.0, and 1.5 m) were accounted for. Under these scenarios, the avalanche path can widely reach the Prati di Tivo area, involving the residence (reported as the hotel in Figure 14) and the four-seat chairlift line (Figures 16b and 17).

Snow avalanches can generally act as geomorphic agents [135]. Snow avalanches can exert considerable erosive forces playing a significant role in landscape development. Evaluating the morphological features of the mass movement-prone area and the main avalanche features is essential to quantify the material entrained by the avalanche and transported to the deposition zone [136].

A semi-quantitative analysis was applied to the modeled avalanche path at Vallone della Giumenta (Figures 13 and 17) to better describe the geomorphic role of snow avalanches at the Prati di Tivo area. This specific site investigation presents peculiar morphometric features and snow avalanche pressures accounted as representative of the main avalanche events in the study area. The analysis focused on evaluating the pre- and post-avalanche setting, highlighting the variations in the contributing area caused by the snow avalanche along the Vallone della Giumenta. This evaluation showed a variation that increased by about two-fold (>50%), as the contribution of each avalanche track and rock gully was significant in the geomorphic action of the avalanche. It is graphically shown in Figure 18 and summarized in Table 4.

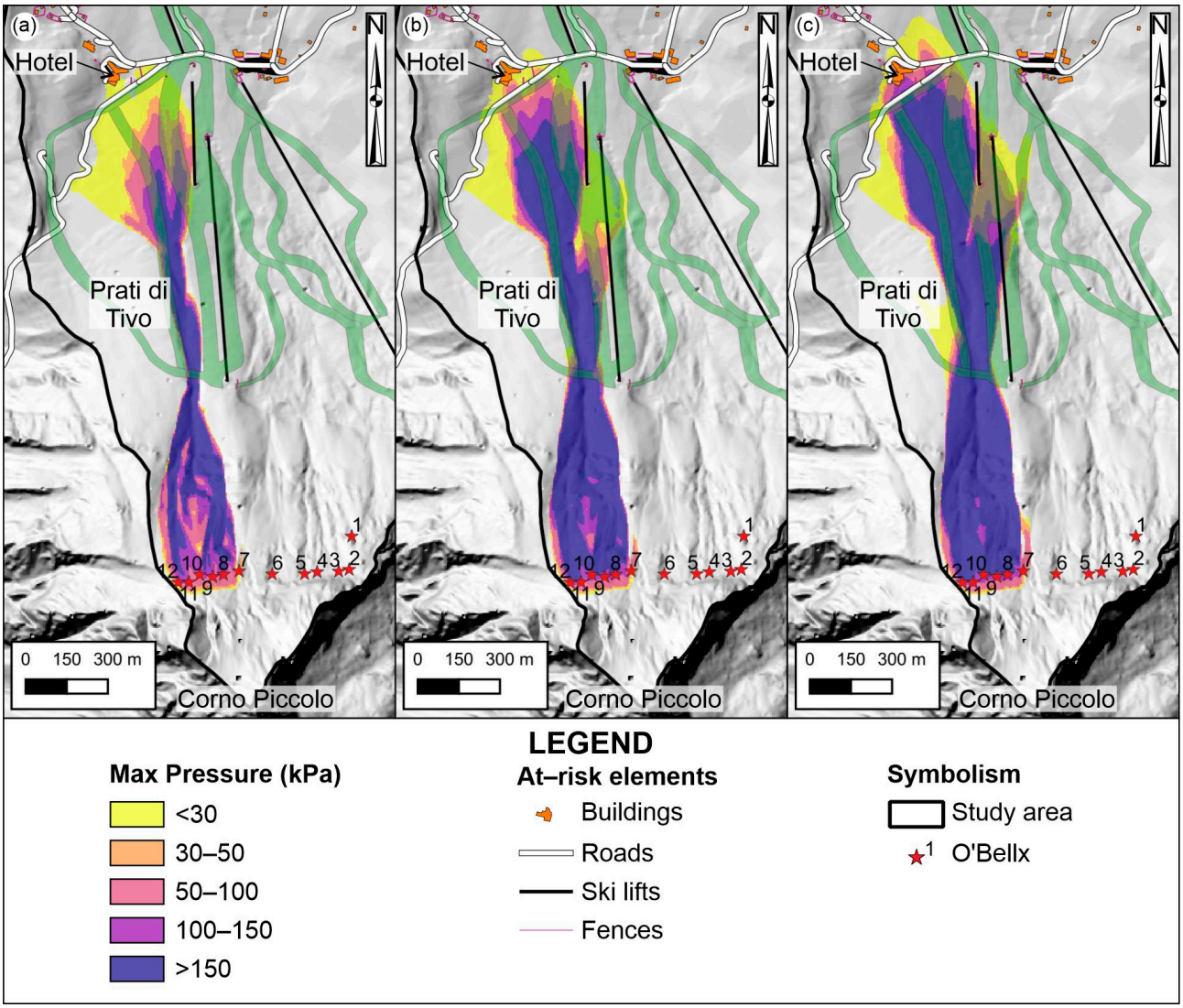

Figure 17. Results of the avalanche dynamics simulation under different transmitted pressures and heights of snow cover: (**a**) Hc = 0.5 m, (**b**) Hc = 1.0 m, and (**c**) Hc = 1.5 m.

In conclusion, the resulting data allowed us to properly define the main steps of the developed risk mitigation protocol. It was activated following some recent damaging snow avalanches affecting the Prati di Tivo area to better develop mitigation activities and land use policies needed for the management of permanent settlements, recreation infrastructures, and ski facilities. The relevance and the impact of the work are represented by: (1) the provision of new data on the physiography–geomorphology of the study area and the mass movement-prone areas, (2) the outline of a multidisciplinary methodological approach for the definition of snow avalanche critical areas and the configuration of hazard protocols not yet developed for the Central Apennines, and (3) a technical scientific basis to develop the civil protection plans required to increase the knowledge of citizens and interested stakeholders about proper land management considering multi-hazard scenarios (i.e., snow avalanches and landslides).

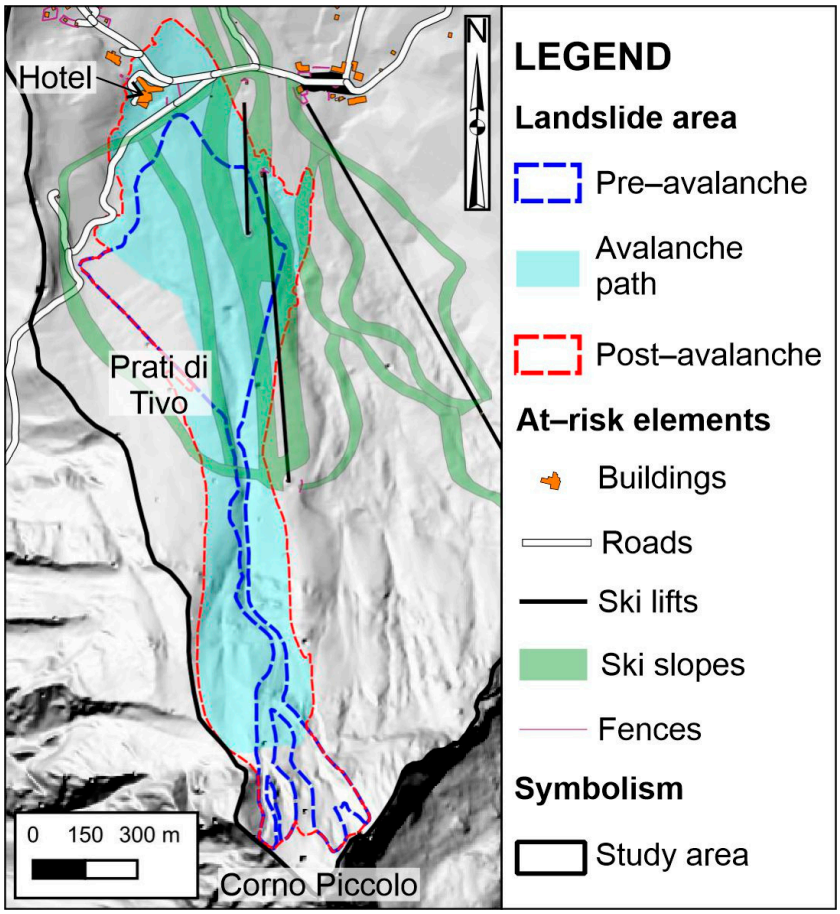

Figure 18. Pre- and post-avalanche landslide contributing area.

Table 4. Dimensions of the possible landslide area, modified by snow avalanche dynamics.

Pre-Avalanche Landslide Area (km^2)	Snow Avalanche Area (km^2)	Post-Avalanche Landslide Area (km^2)
0.363	0.645	0.769

6. Conclusions

Snow avalanches are among the most destructive natural hazards threatening built structures, ski resorts, and landscapes in cold and mountainous regions. The Central Apennines high-mountain environment has been largely affected by different types of mass movements in recent years, accentuated in frequency and magnitude due to changes in the climate regime. The increase in temperatures, the irregularity of intense weather events, and several heavy snowfall events determined an increase in landslide and/or snow avalanche hazards, especially in areas with well-developed tourist facilities.

The Prati di Tivo area has been widely affected by several mass movement phenomena. Like other mountain territories of the Abruzzo Region, the study area is not immune to the general increased tourist fruition and related snow avalanche risk. It is located on the northern slope of the Gran Sasso Massif (Central Italy), showing peculiar meteorological and snow characteristics that differ from the rest of the Alps and Central Apennines. This work allowed us to better define and analyze the geomorphological and climatic features of the study area. The climate extremization results in relation to environmental risk reduction were evaluated by combining different thematic datasets (e.g., morphometric and geomorphological features, climatic and nivological data, technical information, and numerical modeling). In detail, we carried out a snow avalanche hazard assessment to

outline a multidisciplinary methodological approach for defining snow avalanche-critical areas and a technical scientific basis to set up accurate civil protection plans and land management activities. The analysis was performed following a stepwise methodological approach, including the snow avalanche inventory analysis, the analysis and mapping of snow avalanches' paths, the elaboration of a snow avalanche hazard map, and the definition of numerical models.

Recent exceptional snowfall events in the Abruzzo Region (i.e., January 2017 [75,126,127]) caused several damages and injuries in the surrounding Prati di Tivo area. Consequently, the safety services for ski resorts and facilities were updated by installing 12 Obellx® gas exploders [109] to better manage short-term avalanche risks. However, despite the activation of this risk mitigation protocol, the recent snow avalanche event that occurred on 26 March 2020 testified that the local geomorphological dynamics amplified by the climatic extremization that could lead to approximate and insufficient results deriving from planned safety services. Understanding the likely scenarios and consequences of a changing climate on snow avalanche behavior is essential for planning and managing mountain developments. More specifically, the climatic evolution, characterized by further increases of the average winter temperatures and increasingly more irregular and intense snowfalls, could lead to avalanche events of even greater magnitudes compared to what was observed until now and, consequently, will determine a major need for constant updates of the calculations of the new snow avalanche paths.

Combining and integrating morphometric, geomorphological, climatic, and nivological analyses, it was possible to further advance the methodologies for a snow avalanche hazard assessment, defining the existing relationships between climate extremization and environmental risk in a mass-movement prone area, such as Prati di Tivo area. The resulting data also showed that, to perform a complete snow avalanche hazard assessment, it is necessary to consider the geomorphic role of snow avalanches, which can exert considerable erosive forces extending the contributing areas. Finally, a thorough expert-based study would be highly desirable to constantly evaluate the geomorphological and climatic dynamics of the study area. This kind of study can represent a valuable and operative tool for civil protection activities and territorial planning in relation to emergency management and mitigation measures by assuming the potential occurrence of extreme nivological and meteorological scenarios.

Author Contributions: Conceptualization, M.F. and E.M.; methodology, M.F. and E.M; software, C.C., M.C., G.E. and G.P.; validation, E.M. and M.F.; investigation, M.F. and E.M; resources, M.C. and M.F.; writing—original draft preparation, G.P., C.C., G.E. and M.F; writing—review and editing, G.P., M.F. and E.M.; supervision, E.M.; project administration, M.F. and E.M.; and funding acquisition, E.M. All authors have read and agreed to the published version of the manuscript.

Funding: This research and the APC were funded by Enrico Miccadei, the grant provided by Università degli Studi "G. d'Annunzio" Chieti-Pescara.

Institutional Review Board Statement: Not applicable.

Informed Consent Statement: Not applicable.

Data Availability Statement: The data presented in this study are available on request from the author. The data are not publicly available due to privacy. Images employed for the study will be available online for readers.

Acknowledgments: The authors would like to thank the anonymous reviewers that helped to improve the manuscript with their precious and constructive comments. The authors wish to thank the Cartographic Office of the Abruzzo Region by means of the Open Geodata Portal (http://opendata.regione.abruzzo.it/, accessed on 20 December 2020) and the Ministero dell'Ambiente e della Tutela del Territorio e del Mare (http://www.minambiente.it/, accessed on 20 December 2020) for providing the topographic and cartographic data used for this work. Climatic and nivological data were provided by the Functional Center and Hydrographic Office of the Abruzzo Region (Centro Funzionale e Ufficio Idrografico Regione Abruzzo) and the Meteomont service (https://www.sian.it/infoMeteo, accessed on 15 February 2021). The authors are also grateful to the amateur meteorological

association L'Aquila Caput Frigoris (https://www.caputfrigoris.it/, accessed on 12 January 2021) for providing the updated climatic data (year 2020) used for the work.

Conflicts of Interest: The authors declare no conflict of interest.

References

1. Beniston, M.; Farinotti, D.; Stoffel, M.; Andreassen, L.M.; Coppola, E.; Eckert, N.; Fantini, A.; Giacona, F.; Hauck, C.; Huss, M.; et al. The European mountain cryosphere: A review of its current state, trends, and future challenges. *Cryosphere* **2018**, *12*, 759–794. [CrossRef]
2. Guerra, A.J.T.; Fullen, M.A.; Jorge, M.D.C.O.; Bezzerra, J.F.R.; Shork, M.S. Slope Processes, Mass Movement and Soil Erosion: A Review. *Pedosphere* **2017**, *27*, 27–41. [CrossRef]
3. Solari, L.; Del Soldato, M.; Raspini, F.; Barra, A.; Bianchini, S.; Confuorto, P.; Casagli, N.; Crosetto, M. Review of satellite interferometry for landslide detection in Italy. *Remote Sens.* **2020**, *12*, 1351. [CrossRef]
4. Leroueil, S.; Locat, J. Slope movements—Geotechnical characterization, risk assessment and mitigation. In *Geotechnical Hazards*; Maric, B., Lisac, L., Szavits-Nossan, A., Eds.; Balkema: Rotterdam, The Netherlands, 1998; pp. 95–106.
5. Martino, S.; Antonielli, B.; Bozzano, F.; Caprari, P.; Discenza, M.E.; Esposito, C.; Fiorucci, M.; Iannucci, R.; Marmoni, G.M.; Schilirò, L. Landslides triggered after the 16 August 2018 Mw 5.1 Molise earthquake (Italy) by a combination of intense rainfalls and seismic shaking. *Landslides* **2020**, *17*, 1177–1190. [CrossRef]
6. Aleotti, P.; Chowdhury, R. Landslide hazard assessment: Summary review and new perspectives. *Bull. Eng. Geol. Environ.* **1999**, *58*, 21–44. [CrossRef]
7. Glade, T.; Anderson, M.; Crozier, M.J. *Landslide Hazard and Risk*; John Wiley & Sons Ltd.: Chichester, UK, 2012; ISBN 9780470012659.
8. Marsala, V.; Galli, A.; Paglia, G.; Miccadei, E. Landslide susceptibility assessment of Mauritius Island (Indian ocean). *Geosci.* **2019**, *9*, 493. [CrossRef]
9. Peruccacci, S.; Brunetti, M.T.; Gariano, S.L.; Melillo, M.; Rossi, M.; Guzzetti, F. Rainfall thresholds for possible landslide occurrence in Italy. *Geomorphology* **2017**, *290*, 39–57. [CrossRef]
10. Quesada-Román, A.; Fallas-López, B.; Hernández-Espinoza, K.; Stoffel, M.; Ballesteros-Cánovas, J.A. Relationships between earthquakes, hurricanes, and landslides in Costa Rica. *Landslides* **2019**, *16*, 1539–1550. [CrossRef]
11. Tanyaş, H.; van Westen, C.J.; Allstadt, K.E.; Jessee, M.A.N.; Görüm, T.; Jibson, R.W.; Godt, J.W.; Sato, H.P.; Schmitt, R.G.; Marc, O.; et al. Presentation and Analysis of a Worldwide Database of Earthquake-Induced Landslide Inventories. *J. Geophys. Res. Earth Surf.* **2017**, *122*, 1991–2015. [CrossRef]
12. Calista, M.; Miccadei, E.; Piacentini, T.; Sciarra, N. Morphostructural, Meteorological and Seismic Factors Controlling Landslides in Weak Rocks: The Case Studies of Castelnuovo and Ponzano (North East Abruzzo, Central Italy). *Geosciences* **2019**, *9*, 122. [CrossRef]
13. Nadim, F.; Kjekstad, O.; Peduzzi, P.; Herold, C.; Jaedicke, C. Global landslide and avalanche hotspots. *Landslides* **2006**, *3*, 159–173. [CrossRef]
14. Rahmati, O.; Ghorbanzadeh, O.; Teimurian, T.; Mohammadi, F.; Tiefenbacher, J.P.; Falah, F.; Pirasteh, S.; Ngo, P.T.T.; Bui, D.T. Spatial modeling of snow avalanche using machine learning models and geo-environmental factors: Comparison of effectiveness in two mountain regions. *Remote Sens.* **2019**, *11*, 2995. [CrossRef]
15. CRED EM-DAT. The International Disaster Database. Available online: https://www.emdat.be (accessed on 14 February 2021).
16. Statham, G.; Haegeli, P.; Greene, E.; Birkeland, K.; Israelson, C.; Tremper, B.; Stethem, C.; McMahon, B.; White, B.; Kelly, J. A conceptual model of avalanche hazard. *Nat. Hazards* **2018**, *90*, 663–691. [CrossRef]
17. Voiculescu, M.; Ardelean, F.; Török-Oance, M.; Milian, N. Topographical factors, meteorological variables and human factors in the control of the main snow avalanche events in the fĂgĂraŞ massif (Southern carpathians—Romanian Carpathians): Case studies. *Geogr. Pol.* **2016**, *8*, 47–64. [CrossRef]
18. Navarre, J.P. The principles of snow mechanics: The mechanical properties of snow. In Proceedings of the Université Européenne d'été sur les Risques Naturels: Neige et Avalanches; Brugnot, G., Ed.; Cemagref Publications: Chamonix, France, 1992; pp. 75–86.
19. Fort, M.; Cossart, E.; Deline, P.; Dzikowski, M.; Nicoud, G.; Ravanel, L.; Schoeneich, P.; Wassmer, P. Geomorphic impacts of large and rapid mass movements: A review. *Geomorphol. Reli. Process. Environ.* **2009**, *15*, 47–64. [CrossRef]
20. Ghinoi, A.; Chung, C.J. STARTER: A statistical GIS-based model for the prediction of snow avalanche susceptibility using terrain features—Application to Alta Val Badia, Italian Dolomites. *Geomorphology* **2005**, *66*, 305–325. [CrossRef]
21. Borrel, G. La Carte de Localisation Probable des Avalanches. *Mappemonde* **1994**, *94*, 17–19.
22. Gruber, U.; Bartelt, P.; Haefher, H. Avalanche hazard mapping using numerical Voellmy-fluid models. *Publ. Norges Geotek. Inst.* **1998**, *203*, 117–121.
23. Sauermoser, S. Aavalanche hazard mapping—30 years' experience in Austria. In Proceedings of the 2006 International 901 Snow Science Workshop, Telluride, CO, USA, 1–6 October 2006; pp. 314–321.
24. Bründl, M.; Margreth, S. Integrative Risk Management: The Example of Snow Avalanches. In *Snow and Ice-Related Hazards, Risks, and Disasters*; Haeberli, W., Whiteman, C., Shroder, J.F., Eds.; Elsevier Inc.: Oxford, UK, 2015; pp. 263–301; ISBN 9780123964731.
25. Sinickas, A.; Jamieson, B.; Maes, M.A. Snow avalanches in western Canada: Investigating change in occurrence rates and implications for risk assessment and mitigation. *Struct. Infrastruct. Eng.* **2016**, *12*, 490–498. [CrossRef]

26. Mellor, M. Controlled release of avalanches by explosives. In *Advances in North American Avalanche Technology: 1972 Symposium*; Perla, R., Ed.; USDA Forest Service: Washington DC, USA, 1973; pp. 37–49.
27. Gubler, H. Artificial Release of Avalanches by Explosives. *J. Glaciol.* **1977**, *19*, 419–429. [CrossRef]
28. Binger, C.; Nelsen, J.; Olson, K.A. Explosive shock wave compression in snow: Effects of explosive orientation and snowpack compression. In Proceedings of the ISSW 2006. International Snow Science Workshop, Telluride, CO, USA, 1–6 October 2006; Gleason, J.A., Ed.; Montana State University Library: Bozeman, MT, USA, 2006; pp. 592–597.
29. Frigo, B.; Chiaia, B.; Cardu, M. Snowpack effects induced by blasts: Experimental measurements vs theoretical formulas. In Proceedings of the ISSW 2012. International Snow Science Workshop, Anchorage, AK, USA, 16–21 September 2012; Montana State University Library: Bozeman, MT, USA, 2012; pp. 943–947.
30. Johnson, J.B.; Solie, D.J.; Barrett, S.A. The response of a seasonal snow cover to explosive loading. *Ann. Glaciol.* **1994**, *19*, 49–54. [CrossRef]
31. Barbolini, M.; Cordola, M.; Natale, L.; Tecilla, G. Hazard mapping and land use regulation in avalanche prone areas: Recent developments in Italy. In *Recommendations to Deal with Snow Avalanches in Europe*; Hervas, J., Ed.; ISPRA: Rome, Italy, 2003.
32. Gubler, H.; Wyssen, S.; Kogelnig, A. *Guidelines for Artificial Release of Avalanches*; Wyssen Avalanche Control AG: Reichenbach, Germany, 2012; p. 48.
33. Canadian Avalanche Association (CAA). *Technical Aspects of Snow Avalanche Risk Management—Resources and Guidelines for Avalanche Practitioners in Canada*; Campbell, C., Conger, S., Gould, B., Haegeli, P., Jamieson, B., Statham, G., Eds.; Canadian Avalanche Association: Revelstoke, BC, Canada, 2016; p. 126.
34. Choubin, B.; Borji, M.; Hosseini, F.S.; Mosavi, A.; Dineva, A.A. Mass wasting susceptibility assessment of snow avalanches using machine learning models. *Sci. Rep.* **2020**, *10*, 18363. [CrossRef] [PubMed]
35. Jamieson, B.; Margreth, S.; Jones, A. Application and Limitations of Dynamic Models for Snow Avalanche Hazard Mapping. In Proceedings of the International snow science workshop proceedings 2008, Whistler, BC, Canada, 22 September 2008; pp. 730–739.
36. McClung, D.M.; Lied, K. Statistical and geometrical definition of snow avalanche runout. *Cold Reg. Sci. Technol.* **1987**, *13*, 107–119. [CrossRef]
37. Voiculescu, M. Patterns of the dynamics of human-triggered snow avalanches at the Făgăras massif (Southern Carpathians), Romanian Carpathians. *Area* **2014**, *46*, 328–336. [CrossRef]
38. Sharma, S.; Ganju, A. Complexities of avalanche forecasting in western Himalayas—An overview. *Cold Reg. Sci. Technol.* **2000**, *31*, 95–102. [CrossRef]
39. Gruber, U.; Bartelt, P. Snow avalanche hazard modelling of large areas using shallow water numerical methods and GIS. *Environ. Model. Softw.* **2007**, *22*, 1472–1481. [CrossRef]
40. Valero, C.V.; Wever, N.; Bühler, Y.; Stoffel, L.; Margreth, S.; Bartelt, P. Modelling wet snow avalanche runout to assess road safety at a high-Altitude mine in the central Andes. *Nat. Hazards Earth Syst. Sci.* **2016**, *16*, 2303–2323. [CrossRef]
41. Choubin, B.; Borji, M.; Mosavi, A.; Sajedi-Hosseini, F.; Singh, V.P.; Shamshirband, S. Snow avalanche hazard prediction using machine learning methods. *J. Hydrol.* **2019**, *577*, 123929. [CrossRef]
42. Gaume, J.; van Herwijnen, A.; Gast, T.; Teran, J.; Jiang, C. Investigating the release and flow of snow avalanches at the slope-scale using a unified model based on the material point method. *Cold Reg. Sci. Technol.* **2019**, *168*, 102847. [CrossRef]
43. Bühler, Y.; Kumar, S.; Veitinger, J.; Christen, M.; Stoffel, A. Snehmani Automated identification of potential snow avalanche release areas based on digital elevation models. *Nat. Hazards Earth Syst. Sci.* **2013**, *13*, 1321–1335. [CrossRef]
44. Pecci, M.; D'Aquila, P. Zonazione delle aree valanghive a partire dalla suscettibilità al distacco di valanghe. *Neve e Valanghe* **2010**, *69*, 36–47.
45. Yariyan, P.; Avand, M.; Abbaspour, R.A.; Karami, M.; Tiefenbacher, J.P. GIS-based spatial modeling of snow avalanches using four novel ensemble models. *Sci. Total Environ.* **2020**, *745*, 141008. [CrossRef]
46. Romeo, V.; Fazzini, M. La neve in Appennino. Prime analisi su 30 anni di dati nivometeorologici. *Neve e Valanghe* **2008**, *60*, 58–67.
47. D'Alessandro, L.; De Sisti, G.; D'Orefice, M.; Pecci, M.; Ventura, M. Geomorphology of the summit area of the Gran Sasso d'Italia. *Geogr. Fis. Din. Quat.* **2003**, *26*, 126–141.
48. Miccadei, E.; Piacentini, T.; Buccolini, M. Long-term geomorphological evolution in the Abruzzo area, Central Italy: Twenty years of research. *Geol. Carpathica* **2017**, *68*, 19–28. [CrossRef]
49. Piacentini, T.; Miccadei, E. The role of drainage systems and intermontane basins in the Quaternary landscape of the Central Apennines chain (Italy). *Rend. Lincei* **2014**, *25*, 139–150. [CrossRef]
50. Cavinato, G.P.; Miccadei, E. Sintesi preliminare delle caratteristiche tettoniche e sedimentarie dei depositi quaternari della Conca di Sulmona (L'Aquila). *Alp. Mediterr. Quat.* **1995**, *8*, 129–140.
51. Speranza, F.; Adamoli, L.; Maniscalco, R.; Florindo, F. Genesis and evolution of a curved mountain front: Paleomagnetic and geological evidence from the Gran Sasso range (Central Apennines, Italy). *Tectonophysics* **2003**, *362*, 183–197. [CrossRef]
52. Calamita, F.; Satolli, S.; Scisciani, V.; Esestime, P.; Pace, P. Contrasting styles of fault reactivation in curved orogenic belts: Examples from the central Apennines (Italy). *Bull. Geol. Soc. Am.* **2011**, *123*, 1097–1111. [CrossRef]
53. Vezzani, L.; Festa, A.; Ghisetti, F.C. Geology and tectonic evolution of the Central-Southern Apennines, Italy. *Spec. Pap. Geol. Soc. Am.* **2010**, *469*, 1–58. [CrossRef]
54. Cardello, G.L.; Doglioni, C. From Mesozoic rifting to Apennine orogeny: The Gran Sasso range (Italy). *Gondwana Res.* **2015**, *27*, 1307–1334. [CrossRef]

55. Pace, P.; Di Domenica, A.; Calamita, F. Summit low-angle faults in the Central Apennines of Italy: Younger-on-older thrusts or rotated normal faults? Constraints for defining the tectonic style of thrust belts. *Tectonics* **2014**, *33*, 756–785. [CrossRef]
56. Adamoli, L.; Bertini, T.; Chiocchini, M.; Deiana, G.; Mancinelli, A.; Pieruccini, U.; Romano, A. Ricerche geologiche sul Mesozoico del Gran Sasso d'Italia (Abruzzo). II. Evoluzione tettonico-sedimentaria dal Trias superiore al Cretaceo inferiore dell'area compresa tra il Corno Grande e S. Stefano di Sessanio (F. 140 Teramo). *Stud. Geol. Camerti* **1978**, *4*, 7–17.
57. Adamoli, L.; Bertini, T.; Deiana, G.; Pieruccini, U.; Romano, A. Ricerche geologiche sul Gran Sasso d'Italia (Abruzzo). VI. Primi risultati dello studio strutturale della catena del Gran Sasso d'Italia. *Stud. Geol. Camerti* **1982**, *7*, 97–103.
58. Adamoli, L. Evidenze di tettonica di inversione nell'area Corno Grande—Corno Piccolo (Gran Sasso d'Italia). *Boll. Della Soc. Geol. Ital.* **1992**, *111*, 53–66.
59. Carabella, C.; Buccolini, M.; Galli, L.; Miccadei, E.; Paglia, G.; Piacentini, T. Geomorphological analysis of drainage changes in the NE Apennines piedmont area: The case of the middle Tavo River bend (Abruzzo, Central Italy). *J. Maps* **2020**, *16*, 222–235. [CrossRef]
60. Rovida, A.; Locati, M.; Camassi, R.; Lolli, B.; Gasperini, P.; Antonucci, A. *The Italian Earthquake Catalogue CPTI15—Version 3.0*; Istituto Nazionale di Geofisica e Vulcanologia (INGV): Rome, Italy, 2021. [CrossRef]
61. Geurts, A.H.; Whittaker, A.C.; Gawthorpe, R.L.; Cowie, P.A. Transient landscape and stratigraphic responses to drainage integration in the actively extending central Italian Apennines. *Geomorphology* **2020**, *353*, 107013. [CrossRef]
62. Ciccacci, S.; D'Alessandro, L.; Dramis, F.; Miccadei, E. Geomorphologic evolution and neotectonics of the Sulmona intramontane basin (Abruzzi Apennine, Central Italy). *Z. Fur. Geomorphol. Suppl.* **1999**, *118*, 27–40.
63. Giraudi, C. I rock glacier tardo-pleistocenici e olocenici dell'Appennino—Età, distribuzione, significato paleoclimatico. *Quat. Ital. J. Quat. Sci.* **2002**, *15*, 45–52.
64. Pecci, M.; D'Agata, C.; Smiraglia, C. Ghiacciaio del calderone (Apennines, Italy): The mass balance of a shrinking mediterranean glacier. *Geogr. Fis. Din. Quat.* **2008**, *31*, 55–62.
65. Pecci, M.; D'Aquila, P. Geomorphological features and cartography of the Gran Sasso d'Italia massif between Corno Grande-Corno Piccolo and Pizzo Intermesoli. *Geogr. Fis. Din. Quat.* **2011**, *34*, 127–143.
66. Bianchi-Fasani, G.; Esposito, C.; Lenti, L.; Martino, S.; Pecci, M.; Scarascia-Mugnozza, G. Seismic analysis of the Gran Sasso catastrophic rockfall (Central Italy). In Proceedings of the Landslide Science and Practice: Risk Assessment, Management and Mitigation; Mrgottini, C., Ed.; Springer: Berlin, Germany, 2013; pp. 263–267.
67. Gruppo di lavoro. *Gruppo di Lavoro CPTI Catalogo Parametrico dei Terremoti Italiani, 2004 (CPTI04)*; Editrice Compositori: Bologna, Italy, 2004.
68. Chiarabba, C.; Jovane, L.; DiStefano, R. A new view of Italian seismicity using 20 years of instrumental recordings. *Tectonophysics* **2005**, *395*, 251–268. [CrossRef]
69. ISIDe Working Group. *Italian Seismological Instrumental and Parametric Database (ISIDe)*; Istituto Nazionale di Geofisica e Vulcanologia (INGV): Rome, Italy, 2007. [CrossRef]
70. Peel, M.C.; Finlayson, B.L.; McMahon, T.A. Updated world map of the Köppen-Geiger climate classification. Spatial Data Access Tool (SDAT)OGC Standards-based Geospatial Data Visualization/Download. *Hydrol. Earth Syst.* **2007**, *11*, 1633–1644. [CrossRef]
71. Di Lena, B.; Antenucci, F.; Mariani, L. Space and time evolution of the Abruzzo precipitation. *Ital. J. Agrometeorol.* **2012**, *1*, 5–20.
72. Miccadei, E.; Piacentini, T.; Daverio, F.; Di, R. Geomorphological Instability Triggered by Heavy Rainfall: Examples in the Abruzzi Region (Central Italy). In *Studies on Environmental and Applied Geomorphology*; Piacentini, T., Miccadei, E., Eds.; IntechOpen: London, UK, 2012; pp. 45–62.
73. Chiaudani, A.; Antenucci, F.; Di Lena, B. Historical analysis of maximum intensity precipitation(1, 3, 6, 12 hours) in Abruzzo Region (Italy)—Period 1951–2012. In Proceedings of the Agrometeorologia per la Sicurezza Ambientale ed Alimentare; 2013. Available online: http://agrometeorologia.it/documenti/AIAM2013/113-114_Chiaudani.pdf (accessed on 24 October 2020).
74. Piacentini, T.; Galli, A.; Marsala, V.; Miccadei, E. Analysis of soil erosion induced by heavy rainfall: A case study from the NE Abruzzo Hills Area in Central Italy. *Water* **2018**, *10*, 1314. [CrossRef]
75. Piacentini, T.; Calista, M.; Crescenti, U.; Miccadei, E.; Sciarra, N. Seismically induced snow avalanches: The central Italy case. *Front. Earth Sci.* **2020**, *8*, 507. [CrossRef]
76. Smiraglia, C.; Azzoni, R.S.; D'agata, C.; Maragno, D.; Fugazza, D.; Diolaiuti, G.A. The evolution of the Italian glaciers from the previous data base to the new Italian inventory. Preliminary considerations and results. *Geogr. Fis. Din. Quat.* **2015**, *38*, 79–87. [CrossRef]
77. Vergni, L.; Todisco, F.; Di Lena, B.; Mannocchi, F. Effect of the North Atlantic Oscillation on winter daily rainfall and runoff in the Abruzzo region (Central Italy). *Stoch. Environ. Res. Risk Assess.* **2016**, *30*, 1901–1915. [CrossRef]
78. Vergni, L.; Di Lena, B.; Todisco, F.; Mannocchi, F. Uncertainty in drought monitoring by the Standardized Precipitation Index: The case study of the Abruzzo region (central Italy). *Theor. Appl. Climatol.* **2017**, *128*, 13–26. [CrossRef]
79. Di Lena, B.; Curci, G.; Vergni, L. Analysis of rainfall erosivity trends 1980–2018 in a complex terrain region (Abruzzo, central italy) from rain gauges and gridded datasets. *Atmosphere* **2021**, *12*, 657. [CrossRef]
80. Fazzini, M.; Cardillo, A.; Di Fiore, T.; Lucentini, L.; Scozzafava, M. Extreme temperatures in the cold air pool of the central Apennines (Italy): Comparison with those of the Veneto Pre-Alps during winter 2016–2017. In Proceedings of the 34th International Conference on Alpine Meteorology, Reykjavík, Iceland, 19–23 June 2017; pp. 42–47.

81. Fazzini, M.; Giuffrida, A. Une nouvelle proposition quantitative des régimes pluviométriques dans le territoire de Italie: Premiers résultats. In Proceedings of the Climat Urbain, Ville et Architecture—Actes XVIII Colloque Internationale de Climatologie, Genova, Italy, 7–11 September 2005; pp. 361–364.
82. Fazzini, M.; Magagnini, L.; Giuffrida, A.; Frustaci, G.; Di Lisciandro, M.; Gaddo, M. Nevosità in Italia negli ultimi 20 anni. *Neve Valanghe* **2006**, *58*, 24–35.
83. Strahler, A.N. Dynamic basis of geomorphology. *Bull. Geol. Soc. Am.* **1952**, *63*, 923–938. [CrossRef]
84. Ahnert, F. Local relief and the height limits of mountain ranges. *Am. J. Sci.* **1984**, *284*, 1035–1055. [CrossRef]
85. Schweizer, J.; Jamieson, J.B.; Schneebeli, M. Snow avalanche formation. *Rev. Geophys.* **2003**, *41*, 1–25. [CrossRef]
86. Laute, K.; Beylich, A.A. Morphometric and meteorological controls on recent snow avalanche distribution and activity at hillslopes in steep mountain valleys in western Norway. *Geomorphology* **2014**, *218*, 16–34. [CrossRef]
87. Romshoo, S.A.; Bhat, S.A.; Rashid, I. Geoinformatics for assessing the morphometric control on hydrological response at watershed scale in the upper Indus Basin. *J. Earth Syst. Sci.* **2012**, *121*, 659–686. [CrossRef]
88. ISPRA. Geological Map of Italy, Scale 1:50,000, Sheet 349 "Gran Sasso d'Italia". Available online: https://www.isprambiente.gov.it/Media/carg/349_GRANSASSO/Foglio.html (accessed on 28 March 2021).
89. Abruzzo-Sangro Basin Authority. *Geomorphological Map, Scale 1:25,000. Piano Stralcio di Bacino per l'Assetto 1035 Idrogeologico dei Bacini di Rilievo Regionale Abruzzesi e del Bacino del Fiume Sangro. (L.R. 18.05 1989 n.81 e L. 24.08.2001)*; Abruzzo Region: L'Aquila, Italy, 2005.
90. ISPRA IFFI Project—Italian Landslide Inventory. Available online: https://idrogeo.isprambiente.it/app/iffi?@=41.55172525894153,12.57350148381829,1 (accessed on 24 October 2020).
91. ISPRA. AIGEO Aggiornamento ed Integrazione delle Linee Guida della Carta Geomorfologica D'italia in Scala 1:50.000. In *Quaderni Serie III*; Servizio Geologico d'Italia: Rome, Italy, 2018.
92. Smith, M.J.; Paron, P.; Griffiths, J. *Geomorphological Mapping, Methods and Applications*; Elsevier Science: Oxford, UK, 2011; ISBN 9780444534460.
93. Miccadei, E.; Mascioli, F.; Ricci, F.; Piacentini, T. Geomorphology of soft clastic rock coasts in the mid-western Adriatic Sea (Abruzzo, Italy). *Geomorphology* **2019**, *324*, 72–94. [CrossRef]
94. Pasculli, A.; Palermi, S.; Sarra, A.; Piacentini, T.; Miccadei, E. A modelling methodology for the analysis of radon potential based on environmental geology and geographically weighted regression. *Environ. Model. Softw.* **2014**, *54*, 165–181. [CrossRef]
95. Carabella, C.; Miccadei, E.; Paglia, G.; Sciarra, N. Post-Wildfire Landslide Hazard Assessment: The Case of The 2017 Montagna Del Morrone Fire (Central Apennines, Italy). *Geosciences* **2019**, *9*, 175. [CrossRef]
96. Patton, A.I.; Rathburn, S.L.; Capps, D.M. Landslide response to climate change in permafrost regions. *Geomorphology* **2019**, *340*, 116–128. [CrossRef]
97. Gustavsson, M.; Kolstrup, E.; Seijmonsbergen, A.C. A new symbol-and-GIS based detailed geomorphological mapping system: Renewal of a scientific discipline for understanding landscape development. *Geomorphology* **2006**, *77*, 90–111. [CrossRef]
98. World Meteorological Organization (WMO). *Guide to the Implementation of Education and Training Standards in Meteorology and Hydrology*; WMO: Geneve, Switzerland, 2015.
99. Altevie. *Avalanche Risk Defense Zone of Vena Rossa—Gran Sasso d'Italia*; Altevie: L'Aquila, Italy, 2020.
100. Fazzini, M.; Bisci, C.; De Luca, E. Clima e neve sul massiccio del Gran Sasso. *Neve Valanghe* **1999**, *36*, 36–45.
101. Swiss Federai Institute for Snow and Avalanche Research (SLF). *Direttive per la Considerazione del Pericolo di Valanghe Nelle Attività di Incidenza Territoriale*; Swiss Federai Institute for Snow and Avalanche Research SLF: Davos, Switzerland, 1984; p. 22.
102. Salm, B.; Burkard, A.; Gubler, H.U. *Berechnung von Fliesslawinen; eine Anleitung für Praktiker mit Beispielen*; Mitteilungen des Eidgenössischen Institutes für Schnee und Lawinenforschung: Davos, Switzerland, 1990; p. 37.
103. Percitti, G. Avalanche study in Italy. In Proceedings of the European Summer University on Snow and Avalanches, Chamonix, France, 14–25 September 1992; Cemagref Publications: Beaucouze, France, 1992.
104. Chrustek, P.; Kolecka, N.; Bühler, Y. Snow avalanches mapping—Evaluation of a new approach. In Proceedings of the International Snow Science Workshop, Grenoble, France, 7–11 October 2013; pp. 750–755.
105. Brandolini, P.; Faccini, F.; Fratianni, S.; Freppaz, M.; Giardino, M.; Maggioni, M.; Perotti, L.; Romeo, V. Snow-avalanche and climatic conditions in the Ligurian ski resorts (NW-Italy). *Geogr. Fis. Din. Quat.* **2017**, *40*, 41–52. [CrossRef]
106. Barbolini, M.; Pagliardi, M. Analisi costi-benefici applicata alla gestione del problema valanghe: Applicazione ad un caso di studio in Alta Valbrembana (BG). In Proceedings of the Internation Symposion Interpraevent, Riva del Garda, Italy, 24–27 May 2004; pp. 13–24.
107. Cappabianca, F.; Barbolini, M.; Natale, L. Snow avalanche risk assessment and mapping: A new method based on a combination of statistical analysis, avalanche dynamics simulation and empirically-based vulnerability relations integrated in a GIS platform. *Cold Reg. Sci. Technol.* **2008**, *54*, 193–205. [CrossRef]
108. Maggioni, M.; Gruber, U.; Purves, R.S.; Freppaz, M. Potential release areas and return period of avalanches: Is there a relation? In Proceedings of the International Snow Science Workshop, Telluride, CO, USA, 1–6 October 2006; pp. 566–571.
109. Bruno, E.; Maggioni, M.; Freppaz, M.; Zanini, E. *Distacco Artificiale di Valanghe: Linee Guida per la Procedura Operativa Metodi e Normativa*; Regione Autonoma Valle d'Aosta—Région Autonome Vallée d'Aoste: Aosta, Italy, 2012; p. 130.

110. Boccardo, P.; Fissore, V.; Morreale, S.; Ilardi, E.; Baldo, M. Aerial Lidar technology in support to avalanches prevention and risk mitigation: An operative application at "Colle della Maddalena" (Italy). *ISPRS Ann. Photogramm. Remote Sens. Spat. Inf. Sci.* **2020**, *VI-3/W1-20*, 11–17. [CrossRef]
111. Vagliasindi, M.; Theodule, A.; Maggioni, M.; Levera, E. Artificial avalanche release as a protection measure for major roads: The case study of road S.S. 21 "Colle della Maddalena" (CN, Western Italian Alps). In Proceedings of the International Snow Science Workshop, Telluride, CO, USA, 7–11 October 2013; pp. 875–882.
112. Christen, M.; Bartelt, P.; Gruber, U. *Numerical Calculation of Dense Flow and Powder Snow Avalanches*; Swiss Federal Institute for Snow and Avalanche Research (SLF): Davos, Switzerland, 2010; p. 136.
113. Margreth, S. *Costruzione di Opere di Premunizione Contro le Valanghe Nella Zona di Distacco. Direttiva Tecnica: Aiuto all'Esecuzione*; Ufficio federale dell'ambiente (WSL); Istituto Federale per lo Studio della Neve e delle Valanghe (SNV): Davos, Switzerland, 2007; p. 139.
114. Oller, P.; Janeras, M.; de Buen, H.; Arnó, G.; Christen, M.; García, C.; Martínez, P. Using AVAL-1D to simulate avalanches in the eastern Pyrenees. *Cold Reg. Sci. Technol.* **2010**, *64*, 190–198. [CrossRef]
115. Bartelt, P.; Bühler, Y.; Christen, M.; Deubelbeiss, Y.; Salz, M.; Schneider, M.; Schumacher, L. *RAMMS. Avalanche Numerical Model for Snow Avalanches in Research and Practice. User Manual*; Swiss Federal Institute for Snow and Avalanche Research (SLF): Davos, Switzerland, 2017; p. 104.
116. Fischer, J.T.; Kowalski, J.; Pudasaini, S.P. Topographic curvature effects in applied avalanche modeling. *Cold Reg. Sci. Technol.* **2012**, *74–75*, 21–30. [CrossRef]
117. Christen, M.; Bartelt, P.; Gruber, U. AVAL-1D: An avalanche dynamics program for the practice. In Proceedings of the Protection of Habitat against Floods, Debris Flows and Avalanches, Matsumoto, Japan, 14–18 October 2002; pp. 715–725.
118. Christen, M.; Kowalski, J.; Bartelt, P. RAMMS: Numerical simulation of dense snow avalanches in three-dimensional terrain. *Cold Reg. Sci. Technol.* **2010**, *63*, 1–14. [CrossRef]
119. Bisci, C.; Fazzini, M.; Romeo, V.; Cardillo, A. Intense snowfalls of January 2017 along the central-southern Apennines (Italy), in comparisons with the 2015, 2012 and 2005 events. In Proceedings of the 34th International Conference on Alpine Meteorology, Reykjavík, Iceland, 18–23 June 2017; pp. 48–50.
120. Dramis, F.; Fazzini, M.; Pecci, M.; Smiraglia, C. The effects of Global Warming onto the Meditearranean high altitudes: The naturaly laboratory of Calderone Glacier (Central Apennines Italy). In Proceedings of the 32th International Geological Congress (IGC), Florence, Italy, 20–28 August 2004; Abbate, E., Ed.; IUGS, International Union of Geological Sciences: Paris, France; EC, European Commission: Brussels Belgium; pp. 111–117.
121. Bisci, C.; Fazzini, M. *Studio Idraulico-Ambientale Mediante L'analisi dei Processi Geomorfologici in Atto per la Caratterizzazione dei Bacini Idrografici Principali della Regione Marche—Analisi Climatologica*; Consorzio di Bonifica delle Marche: Ancona, Italy, 2019; p. 34.
122. Fazzini, M.; Romeo, V. L'enneigement dans les Apennins durant les derniers 30 ans. In Proceedings of the Actes XXIV Colloque AIC "Climat montagnard et risques"; Stamperia Romana: Roma, Italy, 2011; pp. 249–254.
123. D'Alessandro, L.; Pecci, M. Valanghe sul Gran Sasso d'Italia: Nota preliminare. *Mem. della Soc. Geol. Ital.* **2001**, *56*, 315–320.
124. De Sisti, G.; Monopoli, S.; Pecci, M. Valanghe sul Gran Sasso d'Italia: Analisi delle condizioni meteoclimatiche e implicazioni dell'assetto geomorfologico con particolare riferimento all'attività valanghiva dell'inverno 2002–2003. *Neve Valanghe* **2004**, *52*, 20–33.
125. Barbolini, M.; Pagliardi, M.; Ferro, F.; Corradeghini, P. Avalanche hazard mapping over large undocumented areas. *Nat. Hazards* **2011**, *56*, 451–464. [CrossRef]
126. Issler, D. The 2017 Rigopiano avalanche—dynamics inferred from field observations. *Geosciences* **2020**, *10*, 446. [CrossRef]
127. Braun, T.; Frigo, B.; Chiaia, B.; Bartelt, P.; Famiani, D.; Wassermann, J. Seismic signature of the deadly snow avalanche of January 18, 2017, at Rigopiano (Italy). *Sci. Rep.* **2020**, *10*, 18563. [CrossRef]
128. Ballesteros-Cánovas, J.A.; Trappmann, D.; Madrigal-González, J.; Eckert, N.; Stoffel, M. Climate warming enhances snow avalanche risk in the Western Himalayas. *Proc. Natl. Acad. Sci. USA* **2018**, *115*, 3410–3415. [CrossRef]
129. Strapazzon, G.; Schweizer, J.; Chiambretti, I.; Brodmann Maeder, M.; Brugger, H.; Zafren, K. Effects of Climate Change on Avalanche Accidents and Survival. *Front. Physiol.* **2021**, *12*, 450. [CrossRef]
130. Martin, E.; Giraud, G.; Lejeune, Y.; Boudart, G. Impact of a climate change on avalanche hazard. *Ann. Glaciol.* **2001**, *32*, 163–167. [CrossRef]
131. Castebrunet, H.; Eckert, N.; Giraud, G.; Durand, Y.; Morin, S. Projected changes of snow conditions and avalanche activity in a warming climate: The French Alps over the 2020–2050 and 2070-2100 periods. *Cryosphere* **2014**, *8*, 1673–1697. [CrossRef]
132. Komarov, A.; Seliverstov, Y.; Sokratov, S.; Glazovskaya, T.; Turchaninova, A. Avalanche risk assessment in Russia. In Proceedings of the Geophysical Research Abstracts, EGU General Assembly, Vienna, Austria, 23–28 April 2017; p. 1.
133. Hovelsrud, G.K.; Karlsson, M.; Olsen, J. Prepared and flexible: Local adaptation strategies for avalanche risk. *Cogent Soc. Sci.* **2018**, *4*, 1460899. [CrossRef]
134. Yount, J.M.; Gorsage, B.R. Evolution of an avalanche program: From artillery to infrascructure. In Proceedings of the International Snow Science Workshop; 2016; pp. 442–449. Available online: https://www.slf.ch/fileadmin/user_upload/WSL/Mitarbeitende/schweizj/vanHerwijnen_etal_PTV_ISSW2016.pdf (accessed on 24 October 2020).
135. Luckman, B.H. The Geomorphic Activity of Snow Avalanches. *Geogr. Ann. Ser. A Phys. Geogr.* **1977**, *59*, 31–48. [CrossRef]
136. Freppaz, M.; Godone, D.; Filippa, G.; Maggioni, M.; Lunardi, S.; Williams, M.W.; Zanini, E. Soil erosion caused by snow avalanches: A case study in the Aosta Valley (NW Italy). *Arctic Antarct. Alp. Res.* **2010**, *42*, 412–421. [CrossRef]